RICE UNIVERSITY

Polysulfone Ultrafiltration Membranes Impregnated with Silver Nanoparticles Show Improved Biofouling Resistance and Virus Removal

by

Katherine Rey Zodrow

A THESIS SUBMITTED
IN PARTIAL FULFILLMENT OF THE
REQUIREMENTS FOR THE DEGREE

Master of Science

APPROVED, THESIS COMMITTEE:

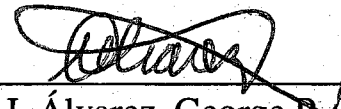

Pedro J.J. Álvarez, George R. Brown
Professor, Chair
Civil and Environmental Engineering

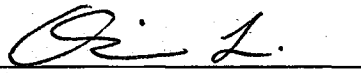

Qilin Li, Assistant Professor
Civil and Environmental Engineering

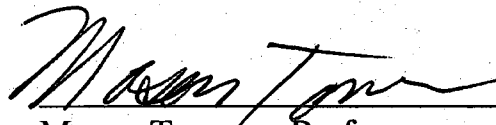

Mason Tomson, Professor
Civil and Environmental Engineering

HOUSTON, TEXAS
MAY 2009

ABSTRACT

Polysulfone Ultrafiltration Membranes Impregnated with Silver Nanoparticles Show Improved Biofouling Resistance and Virus Removal

by

Katherine Rey Zodrow

Biofouling and virus penetration are two significant obstacles in water treatment membrane filtration. Biofouling reduces membrane permeability, increases energy costs, and decreases the lifetime of membranes. In order to effectively remove viruses, nanofiltration or reverse osmosis (both high-energy filtration schemes) must be used. Thus, there is an urgent demand for low-pressure membranes with anti-biofouling and anti-viral properties. The antibacterial properties of silver are well known, and silver nanoparticles (nAg) are now incorporated into a wide variety of consumer products for microbial control. In this study, nAg incorporated into polysulfone ultrafiltration membranes (nAg-PSf) exhibited antimicrobial properties towards a variety of bacteria, including *Escherichia coli* K12 and *Pseudomonas mendocina* KR1, and enhanced the removal of MS2 bacteriophage. Nanosilver incorporation also increased membrane hydrophilicity, reducing the potential for other types of membrane fouling. Thus, the incorporation of nAg into polysulfone ultrafiltration membranes increases both membrane efficiency and effectiveness.

ACKNOWLEDGEMENTS

The work detailed in this thesis could not have been completed without the help of many individuals. Although it would be impossible to mention everyone who has influenced this research in some form, I will acknowledge those who, without their help, this project would have never come to fruition. Dr. Pedro Alvarez, my advisor and thesis committee chair, whose introductory environmental engineering course first got me interested in environmental engineering, helped guide me through this project. He has been a constant source of good advice and motivation. Dr. Qilin Li, my co-advisor, who has helped me learn not only about membrane filtration but also about other forms of water treatment, is a continuous source of helpful advice, interesting ideas, and inspiration. I would also like to thank Dr. Mason Tomson, my third committee member, for his assistance and insight.

I greatly appreciated the help of many people in the lab. Most especially towards the end of this project, Dr. Shaily Mahendra's help has been crucial. In addition to assisting in chemical analysis, she has offered a much-appreciated critical eye for the development of this research. My interest in this particular subject was aided by Dr. Léna Brunet, who I worked closely with when I first came to the Alvarez lab and who taught me many of the techniques needed for membrane analysis. I would also like to thank Dr. Delina Lyon, who taught me many of the microbial laboratory techniques I used in this project and was always there when I needed help designing an experiment. I would like to thank Dong Li, Michael Liga, and Anna Zhang for their help with the virus-

related sections of this work, and I would like to thank Zoltan Krudy and Mark Hoffman, undergraduates in our lab, for their help with experiments. Erika Bryant aided the project with her help with the TEM analysis. Angelo Bendetto and William Deery provided much needed aid in training me in microscopy techniques. I would like to thank those who funded this project - EPA-STAR R832534 and the NSF-funded Center for Biological and Environmental Nanotechnology.

I thank all of the other members of the Alvarez Lab, the Civil and Environmental Engineering Department, and all of my other friends for their intellectual and moral support. I would also like to thank Sandra Baylor, Marilu Campos, Andrea Torres, and Emily Hall – this department would accomplish nothing without them. Most importantly, I would like to thank my family because without them, I would never be where I am today. I have grown a lot in my time at Rice, and none of this would ever have been possible if it were not for everyone listed here.

TABLE OF CONTENTS

LIST OF FIGURES AND TABLES

1.0 INTRODUCTION

As the world's population grows, it becomes increasingly difficult to provide populations with safe drinking water. Today, more than 1 billion people do not have access to safe drinking water, with a mere 3% of the Earth's readily available water existing as fresh water. Water is essential to life, and as it becomes more and more scarce, people look towards non-conventional water treatment technologies like membrane filtration to meet increasingly strict water quality standards and ever-growing water supply needs. Membrane technologies provide a reliably pure permeate with a much smaller land footprint than conventional water treatment processes. Thus, the membrane industry is growing rapidly, providing systems for drinking water treatment, wastewater treatment, industrial water treatment, and desalination.

One major problem faced by the membrane industry is membrane fouling. As water is filtered through membranes, impurities and microorganisms collect and grow on the membrane's surface, decreasing membrane flux and increasing energy costs. In addition to fouling issues, the low-pressure membrane industry experiences difficulty in obtaining 4-log removal of viruses, as required by the Surface Water Treatment Rule, without the use of pretreatment processes (2007). The addition of nanomaterials to water filtration membranes can potentially solve both of these problems.

Project objectives:

1. Develop a water treatment membrane that is resistant to biofouling and enhances virus removal through the incorporation of nanomaterials.

2. Characterize this modified membrane to determine how this nanomaterial alters membrane properties.
3. Quantify the biofilm reduction and virus removal potential of this membrane and how these properties change with water filtration.
4. Explore the potential mechanisms of biofouling reduction and virus removal.

This research explored the effectiveness of many different nanomaterials additives to polysulfone membranes, including multi-walled carbon nanotubes, fullerenes, fullerenes coated with poly(vinyl pyrrolidone), and silver nanoparticles. Among all nanomaterials initially tested, nanosilver showed the most promise as an anti-biofouling agent.

Hypothesis: The addition of nanosilver particles to a polysulfone ultrafiltration reduces biofouling through the antimicrobial action of silver nanoparticles and cations and enhances virus removal efficiency of MS2 through virus interactions with silver nanoparticles and the antiviral action of silver ions.

The preliminary research (detailed in Part I) identified silver nanoparticles (or nano-silver, nAg) as the most promising membrane additive for biofouling reduction. Thus, nAg impregnation of polysulfone membranes was explored in depth in Part 2. After a summary of the literature (in the areas of water treatment membranes, antibacterial nanomaterials, and the use of these nanomaterials in water treatment and water treatment membranes), the results of this detailed study are presented. Following the results are the implications of this research and the needs for future research.

PART 1:

A SURVEY OF ANTIMICROBIAL PROPERTIES OF MEMBRANES WITH NANOTUBES, C_{60} DERIVATIVES, AND PRELIMINARY nAg EXPERIMENTS

Before nAg-PSf membranes were fabricated for the experiments mentioned in Part 2, many experiments were carried out to determine the effectiveness of several membranes with incorporated nanomaterials as biofouling-reducing agents. Nanoparticle additions to these membranes included multi-walled nanotubes (Brunet et al., 2008), buckminsterfullerenes (free suspension - nC_{60}, and coated with PVP – PVP/C_{60}), and nanosilver (nAg). These membranes were characterized and tested for bactericidal propertiess. The methods, results, and implications of these preliminary experiments are briefly summarized in Part 1. Among all of the compounds tested, nAg showed the most promise as an antibacterial agent and was therefore chosen for the more extensive study discussed in Part 2.

2.0 REVIEW OF CNTs AND C_{60} AS POTENTIAL MEMBRANE ADDITIVES*

2.1 Properties of carbon nanutubes and carboxylated carbon nanotubes

One potential advantage of the use of carbon nanotubes (CNT) composites for water treatment is the possibility that the toxicity of particular fullerenes towards bacteria might be exploited when they are dispersed in membranes. Currently, most of the toxicological evaluations conducted on cultured cells or *in vivo* support the toxicity of CNTs (Ding and Liu, 2005; Lam et al., 2006) although the antimicrobial response depends on the degree of sidewall functionalization (Sayes et al., 2006). Although the toxicity of CNTs towards prokaryotes may be different than CNT toxicity towards eukaryotes, one study showed that multi-walled carbon nanotubes (MWCNTs) caused cell death and apoptosis with corresponding changes in the protein expression of human skin fibroblasts; however, this study did not conclusively define the mechanism of cell death (Ding and Liu, 2005). Another study with *Escherichia coli* demonstrated that MWCNTs are able to form temporary "nanochannels" in the cell membrane, which lead to a decrease in cell viability (Rojas-Chapana et al., 2005). Given the antimicrobial effects of nanotubes, CNTs immobilized within the membrane skin might serve as a basis for inhibiting bacterial growth and reducing biofouling. Narayan et al. successfully manufactured carbon nanotube composite films with antibacterial properties in the hopes of reducing biofilm

*The information presented here concerning the incorporation of CNT into polysulfone membranes was previously published in: Brunet, Lyon, Zodrow, Rouch, Caussat, Serp, Remigy, Wiesner, and Alvarez, 2008. Properties of membranes containing semi-dispersed carbon nanotubes. Environmental Eng Sci 25, 565-576.

formation (Narayan et al., 2005). More recently, CNT have been deposited onto a filter to improve removal of viruses and bacterial pathogens (Brady-Estevez et al., 2008). Here, we examine the effectiveness of CNT immobilized within a polysulfone membrane for biofouling reduction.

2.2 *Properties of nC_{60}*

Although fullerene molecules are hydrophobic and relatively insoluble, they can be dispersed in solution over long periods of stirring or sonication, thus being made bioavailable to bacteria in suspension (Fortner et al., 2005; Lyon et al., 2005a). An aqueous dispersion of C_{60} (nC_{60}) is essential for utilization of its antibacterial effects. In addition to manual dispersion in water, fullerenes can be solubilized through the use of a polymer (e.g. PVP) or a surfactant, and fullerenes dispersed in this manner may retain their antimicrobial properties. For example, the minimum inhibitory concentration of PVP/C_{60} is approximately 0.6 – 1.0 mg/L for *E. coli* (Lyon et al., 2006).

The dispersion medium greatly affects the antimicrobial activity of the fullerene. For example, fullerenes in Luria-Bertani broth will precipitate out of solution or be coated by proteins present in the media, thus becoming unavailable for interactions with bacteria (Fortner et al., 2005). Therefore, a minimal media was chosen for the following study.

The mechanism of toxicity of these particles is related to oxidative stress caused by C_{60} aggregates on the cell wall. For example, *Pseudomonas putida* exposed to a fullerene suspension were observed to have decreased levels of unsaturated fatty acids and increased levels of cyclopropane fatty acids in their cell membrane, making them less

susceptible to oxidation (Fang et al., 2007). At sufficient concentrations (as low as 0.1 mg/L for small nC_{60} aggregates), damage induced on the cell wall increased the cell's susceptibility to osmotic stress and inhibited nutrient uptake, leading to cell death (Lyon et al., 2006). This oxidative stress on the cell wall was not due to the production of reactive oxygen species (ROS) by the fullerene aggregates because this antimicrobial effect was also observed in both anaerobic and dark conditions (Lyon et al., 2005b).

Although few have studied the addition of fullerenes to water treatment membranes for biofouling reduction, fullerenes have been added to water treatment membranes for the enhancement of membrane properties. Fullerene C_{60} and astralene (a material that contains between 20 and 90% by weight nanoparticles) were added to ultrafiltration membranes (Ong et al., 2006; Polotskaya et al., 2007). These membranes experienced good water flux restoration after contact with a protein mixture (compared to the control), and a decrease in sorption capacity for proteins with no significant change in the membrane pore structure (Polotskaya et al., 2007). Additionally, fullerenes have been added to polymeric membranes to increase the rejection of estrogenic compounds (Ong et al., 2006). Thus, C_{60} may be a very useful membrane additive.

3.0 MATERIALS AND METHODS

3.1 Fabrication of CNT membranes

Polysulfone beads (PSf -UDEL® P3500) were provided by Solvay (Brussels, Belgium). *N*-Methyl-2-pyrrolidone (NMP), used as PSf solvent, and poly(vinyl pyrrolidone) (PVP, 10 kDa), used as porogen, were purchased from Aldrich (Lyon, France). The CNTs were produced using a catalytic fluidized bed CVD process developed by B. Caussat (LGC, Toulouse, France) and P. Serp (LCC, Toulouse, France) (Corrias et al., 2003; Morancais et al., 2007). The MWCNTs were then purified with sulfuric acid in order to remove the catalyst, which consisted of iron supported by alumina particles. After this treatment, all the alumina was dissolved and less than 2% w/w of iron remained, as deduced from TGA analyses coupled with SEM/EDAX observations (Morancais et al., 2007). The MWCNTs synthesized consistently displayed an external diameter of 10–40 nm corresponding to 7–16 walls; the tube length was as long as 50 μm.

Membranes were made using the wet phase inversion process. The polymer solution was prepared by first mixing CNTs with NMP using a Polytron PT 1300 D homogenizer (Fisher Scientific Bioblock, Illkirch, France) at 23,000 rpm for 10 min. Then PVP and polysulfone were successively added and mixed at 70°C over 20 h to obtain a homogeneous solution. For both blend solutions, 20% w/w of PSf and 15% w/w of PVP were used. The amount of NMP and CNT added was adjusted as a function of the desired composition: 65% w/w of NMP for the pure polymer membrane, and 63.6 and 1.4% w/w of NMP and CNTs, respectively, for the nanocomposite. The polymer

solutions were deposited in a thin film on a glass plate at room temperature (20°C) with an aluminum casting knife. Three minutes after the casting, the glass plate with polymer solution film was immersed in a water bath at room temperature (20°C), tap water being used as a nonsolvent of the polymer. No CNTs were visually observed in the coagulation bath indicating that CNTs were incorporated into the membrane. The CNT content in the final produced membrane was calculated to be 4% w/w, as the ratio of CNTs to the polymers (PVP and PSf), assuming that all of the solvent was released to the water.

3.2 Fabrication of membranes incorporating C_{60}

Fullerenes, C_{60}, were either added in powder form (0.03% or 0.32% by weight) directly into the casting solution or stabilized with poly(vinyl pyrrolidone). In order to make C_{60} stabilized with PVP (or PVP/C_{60}), 25 mL of 1 g/L C_{60} in toluene was added to 100 mL of chloroform with 0.31% PVP. This solution was allowed to evaporate overnight, leaving a thin film of PVP/C_{60}. The total C_{60} concentration in the PVP/C_{60} membrane was 0.037% w/w.

Polysulfone membranes were produced using the wet phase inversion process, incorporating various nanomaterials into the membrane casting solution. First, the polysulfone solvent *N*-methyl-2-pyrrolidone (NMP) was mixed with the nanoparticles (C_{60} or PVP/C_{60}) in a glass bottle with a stir bar at 50°C. Then the polysulfone beads (PSf -UDEL® P3500, provided by Solvay; Brussels, Belgium) and the porogen poly(vinyl pyrrolidone) (PVP, 10kDa) (purchased from Aldrich; Lyon, France) were added to the solution and mixed at 120°C over 3 days to obtain a homogeneous solution. This polymer solution was subsequently cast onto a glass plate at room temperature

(approximately 20°C) with an aluminum casting knife and submerged in a deionized water bath.

The method of C_{60} insertion was also considered. Because bacteria were most likely to contact the membrane on the membrane's selective surface, after one polysulfone membrane was caste onto the glass plate, an aqueous suspension of C_{60} (nC_{60}) was sprayed onto it. Then, the film was placed in the water coagulation bath. The membrane prepared in this way was referred to as "Surface-C_{60}".

The application of C_{60} onto a commercial polysulfone was also tested. Here, nC_{60} was deposited directly onto the surface of a commercial polysulfone ultrafiltration membrane (Tuffryn; Pall Corporation, 0.2 μm). Two different methods of deposition were used, an airbrush and a pipet (referred to as "a/p"). While the airbursh method offered a very uniform dispersion of nanoparticles on the membrane surface, many of the nanoparticles were lost during the application process. Although fewer particles were lost using the pipet method, the dispersion onto the membrane surface was not uniform. In each procedure, approximately 1 mg of nC_{60} was deposited directly onto the surface of commercial polysulfone membrane. Because these nanoparticles were deposited directly on the surface of the membrane they were potentially more bioavailable than nanoparticles inserted into the membrane casting solution.

3.3 Fabrication of membrane with nAg

One membrane made with nAg is discussed here. In order to observe the effects of nAg deposited directly onto the membrane surface, a water suspension with a total of 1 mg nAg was deposited onto a membrane. Both the pipet and airbrush methods were tested.

A summary of all of the membranes discussed in this series of experiments is given in Table 3.1.

Table 3.1: Summary of nanoparticle additives to membranes. The nanoparticles that were added using the pipet or airbrush technique are indicated with "p/a".

Nanoparticle Additive	**Percent by Weight**
Multi-walled Carbon Nanotubes	4
Carboxylated Carbon Nanotubes	4
C_{60} (high concentration)	0.32
C_{60} (low concentration)	0.03
Surface-C_{60}	Unknown
Surface-C_{60} (p/a)	1
Surface-nAg (p/a)	1

3.4 *Bacteria-membrane interactions*

The antibacterial activity of CNTs incorporated into membranes against the Gram-negative bacterium *Escherichia coli* K12 (ATCC 10798) was assessed. To investigate the effect of CNTs on bacterial growth and adhesion on membranes, two complementary techniques were used. The membranes were either placed on agar plates with bacteria deposited by filtration or immerged in a batch culture of stressed cells. Bacteria were maintained either in Luria Bertani (LB) broth or on LB plates at 37°C. Where noted, a defined medium termed minimal Davis medium (MD) was used (Lyon et al., 2005b).

3.5 *Growth of* E.coli *on agar-supported membranes*

An overnight culture of *E. coli* K12 in LB was diluted in MD to a working OD_{600} of 0.001 and then serially diluted to obtain a final dilution of 10^{-8} in 3-mL MD media. The 3-mL cell suspensions were filtered onto membranes that had been autoclaved in water, with the selective skin layer side up, using a dead-end filtration cell. The membranes were placed onto LB agar plates and incubated at 37°C overnight. The plates were visually evaluated for growth. This test was performed in triplicate.

3.6 *Adhesion and growth of a suspension of* E.coli *on membranes*

Coupons cut from the membranes were immersed in a stationary phase culture of *E. coli* K12 in MD for 3 h. The membranes were then rinsed in water prior to differential staining using 5-cyano-2,3-ditolyl tetrazolium chloride, CTC, and 4_,6-diamidino-2-

phenylindole, DAPI (Huang et al., 1995). DAPI stained the nucleic acids of all the bacteria attached to the membrane, and CTC stained only cells that were actively respiring (i.e., alive). Briefly, the membrane coupons were stained with 0.05% CTC solution for 30 min, the stain was discarded, and the coupons were fixed with 5% formalin. The formalin was removed, the coupons were rinsed, and then they were stained with 1 g/mL DAPI for 5 min. The coupons were removed from the staining solution, rinsed with water, and then mounted on a glass slide with a coverslip secured with tape to immobilize the membrane. The coupons were viewed immediately using an Axioplan 2 imaging fluorescent microscope (Carl Zeiss MicroImaging, Inc.; Thornwood, NY). To ensure the stains were functioning efficiently, bacteria killed with hydrogen peroxide were stained and examined. Cells that were only stained with DAPI were considered dead, while those stained with both DAPI and CTC were considered alive. The number of live and dead cells were counted and compared for eight samples of each membrane type.

3.7 Statistical analysis

Where applicable, standard deviations (SD) and numbers of replicate experiments performed (n) are included. A student *t*-test was used to assess whether differences in membrane properties with and without nanomaterials were significant at the 95% confidence level.

4.0 RESULTS OF PRELIMINARY EXPERIMENTS

4.1 Growth of E. coli *on agar-supported CNT membranes*

Antibacterial activity of the CNTs in the membrane was qualified as a function of growth of *E. coli* that had been filtered onto the membrane surface. In this experiment, the appearance of colonies on both the control membrane and the membrane with 4% CNT confirmed that their growth had not been inhibited (Figire 4.1). The mean colony-forming unit (CFU) counts were not statistically different at the 95% confidence level, with the control having a mean CFU count of 93.5 ± 7.7 and the 4% CNT having a mean CFU count of 125 ± 25.5. With this protocol and the high pressures involved for the filtration, bacteria were forcibly adhered to the membrane surface; thus, the adherence of the bacteria to the membrane was not an issue. The growth of bacteria indicates that carbon nanotubes do not provide antibacterial properties to the membranes.

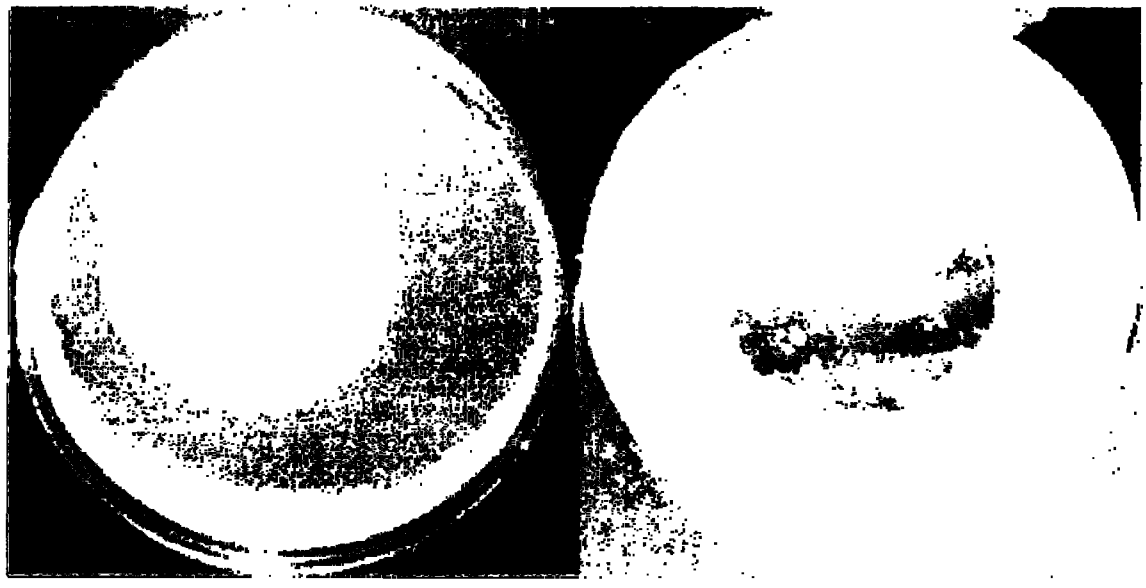

Figure 4.1 Growth of bacteria on the membrane without CNTs (left) and with 4% of CNTs (right). Each membrane disc had an area of 9 cm^2 (Brunet et al., 2008).

4.2 Adhesion and growth on CNT membranes in an E. coli *suspension.*

To assess the biofouling potential of the membranes, the attachment and viability of *E. coli* to their surface was monitored using fluorescent microscopy. While DAPI stained all bacteria present, CTC stained only the respiring cells. Figure 4.2 illustrates a typical pattern of live and dead bacteria, stained by one or both the dyes, and grown on the membrane with 4% of CNT. After immersion for 3 h in a culture of nutrient-deprived cells, *E. coli* were able to adhere to the surface of the membranes and remain respiring. To verify the lack of antibacterial activity afforded by the addition of CNT, the number of live versus dead bacteria was counted.

Very few dead cells were detected (8.6 ± 5.8 % on the control membrane and 7.8 ± 7.4 % on the membrane with CNTs). Over 500 bacteria were counted in total. However, images taken did not necessarily display all the bacteria present on the rough membrane but only those in the same focal plane. For this reason, the total number of cells adhered to the membrane was not quantified. Therefore, we could not verify whether the CNTs would induce a proliferation of the bacteria due to the increased membrane roughness. In summary, these results indicate that CNTs and membranes with immobilized CNTs did not display antibacterial activity. Additionally, the dispersion of the CNTs in the polysulfone membranes did not enhance the growth of bacteria despite the increase membrane roughness. However, this should be confirmed by more extensive tests. We doubt that CNTs are ineffective on account of their concentration in the skin layer (see Figure 4.4) or because the polymer wrapping altered their bioavailability. Instead, the experiments performed with CNTs in a Luria-Broth suspension suggested

that either the CNTs were themselves not antibacterial or their insolubility resulted in a lack of bioavailability and thus no antibacterial activity.

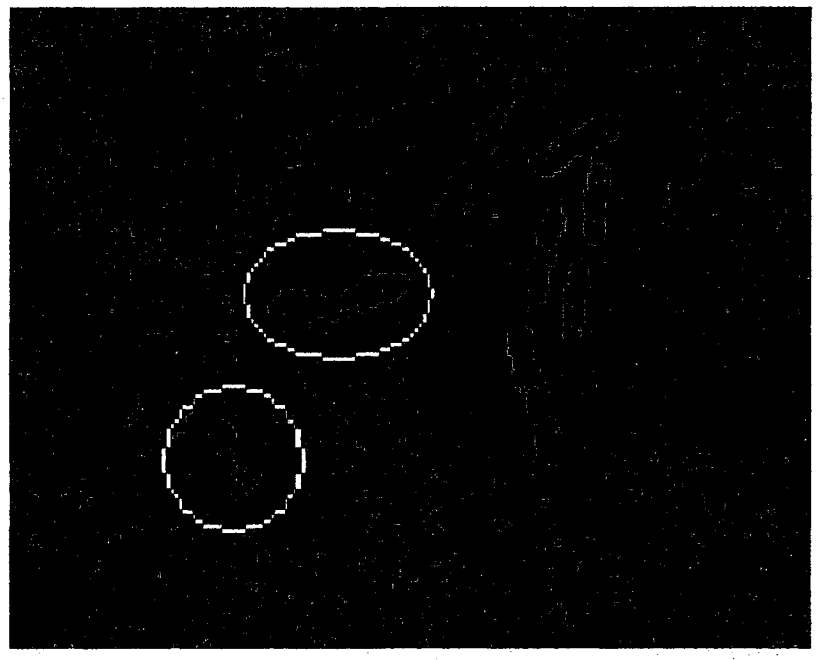

Figure 4.2: Image of live and dead bacteria on a membrane surface. Live bacteria, stained with both CTC and DAPI appears purple (top circled cell) while dead bacteria, stained only with DAPI, appears blue (bottom circled cell).

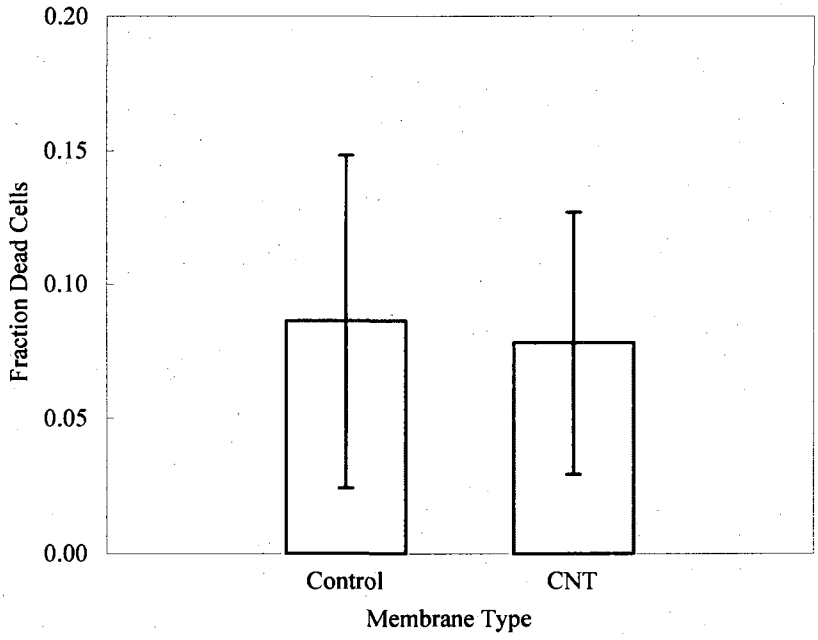

Figure 4.3: Percentage of dead cells on surface of membrane. Membranes displayed are the polysulfone control and 4% CNT. With these particular membranes, the cell death does not vary significantly from the control. Error bars indicate 95% confidence interval levels.

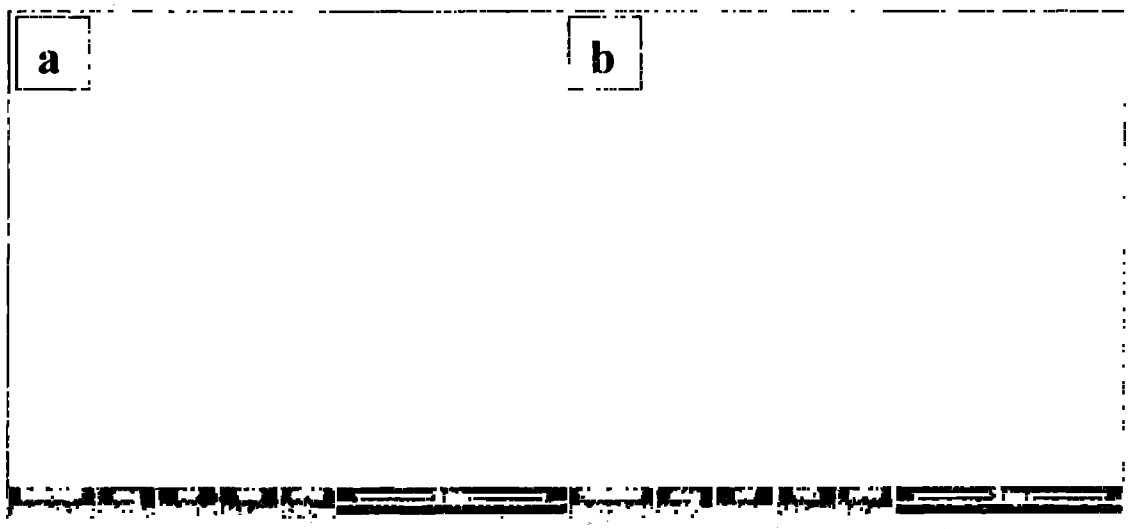

Figure 4.4: High magnification images of membrane surface of control membrane (a) and membrane made with CNT (b) (Brunet et al., 2008).

4.3 Growth of E. coli *on agar-supported nC_{60} membranes*

Bacteria in MD diluted to OD_{600} 10^{-8} were filtered onto the membrane surface of polysulfone nanofiltration membranes made with high and low (0.3% and 0.32%, respectively) concentrations nC_{60}. In this experiment, no significant difference between these membranes and the control was observed (see Figure 4.5), indicating that the concentration of C_{60} added to the membrane casting solution did not lead to a sufficient surface concentration of the compound for the membrane to exhibit antimicrobial properties. Additionally, when a suspension of C_{60} was sprayed onto the membrane surface (Surface-C_{60}), bacterial growth was not inhibited. It is possible that in this sample the C_{60} was either not present in sufficient concentrations for the membrane to exhibit an antimicrobial effect or that the C_{60} disassociated from the membrane surface when the thin polymer film was placed in the coagulation bath. The growth of bacteria on these membranes nC_{60} indicates that, when added to the membrane using this procedure, these additives do not provide antimicrobial properties. Thus, although nC_{60} possesses potent antimicrobial properties in suspension, the C_{60} is not bioavailable to the bacteria at a sufficient antimicrobial concentration when it is incorporated into the polysulfone membrane using this method.

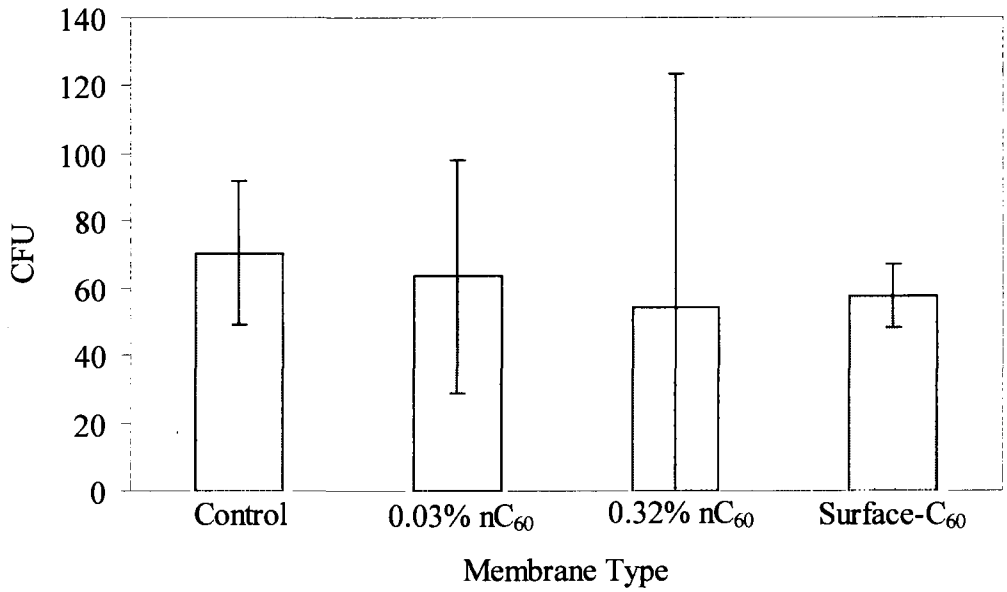

Figure 4.5: Growth of *E. coli* on agar-supported membranes. Polysulfone membranes made with indicated nanoparticles with 95% confidence intervals as defined using the student t-test. Each membrane disk had an area of 9 cm^2.

4.4 Attachment of E. coli *suspension onto C_{60} membranes*

Membranes were placed in a suspension of *E. coli* for a total of 3 hours. After suspension, the membrane coupons were viewed to observe live and dead cells. In this particular case, background staining of CTC was too high for an accurate count of live vs. dead cells. However, the total number of cells attached to the membrane (as observed with the DAPI stain) was quantified (Figure 4.6). The presence of surface-nC_{60} and PVP/C_{60} significantly decreased the number of cells attached to the membrane ($p < 0.05$). The presence of uncoated C_{60} in the membrane significantly increased the number of cells attached to the membrane (perhaps due to an increase in membrane roughness). This experiment indicated that the addition of PVP/C_{60} and C_{60} attached to the surface to reduce biofouling. However, the large difference in bacteria attachment to the C_{60} and surface-nC_{60} membrane is contradictory. It is possible that the C_{60} deposited onto the surface of the surface-nC_{60} membrane was not strongly attached to the surface. Thus, when the membrane was placed in the *E. coli* suspension for 3 hours, some of the surface-nC_{60} detached and entered the suspension, confounding the results.

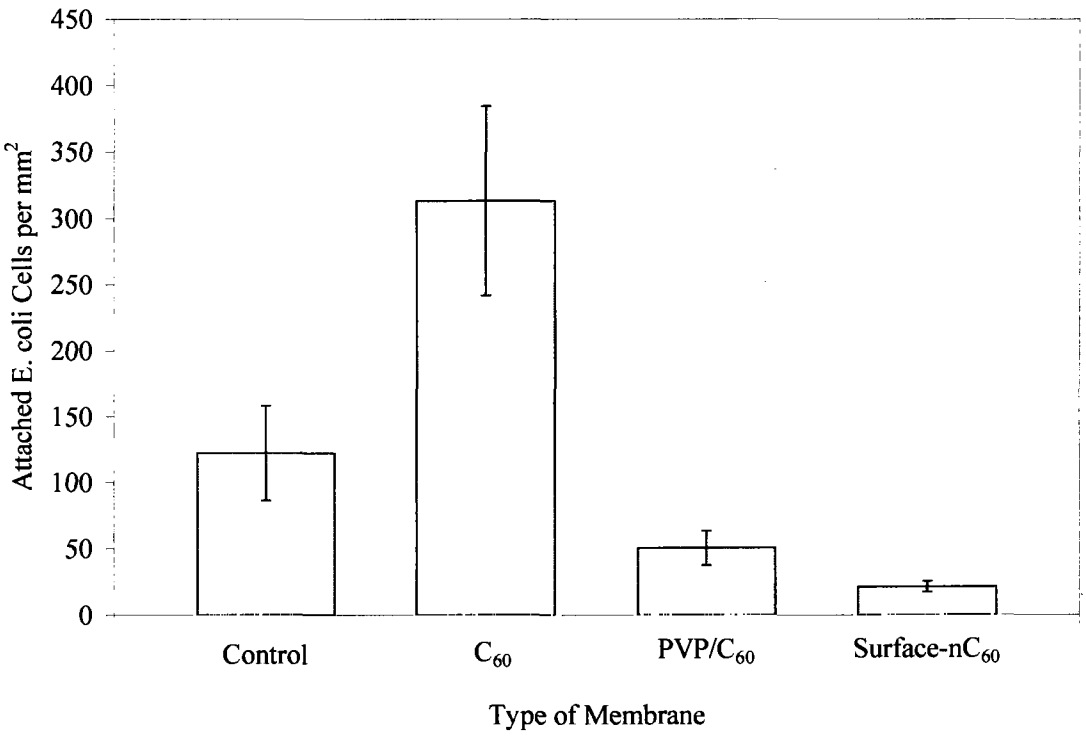

Figure 4.6: Attachment of *E. coli* onto surface of membrane. Cells counts were obtained with cells stained only with DAPI. Both PVP/C_{60} and surface-deposited C_{60} membranes experienced decreased cell attachment. Error bars represent 95% confidence intervals.

4.5 Bacterial growth on membranes with C_{60} and nAg on surface

Some antimicrobial properties were exhibited on commerical polysulfone membranes with 1 mg of nC_{60} and nAg deposited on the surface. Patches of higher particle concentration exhibited less cell growth (see Figure 4.7). Cell counts were performed for each of these membranes and are displayed in Figure 4.8. Although the total number of bacteria filtered onto the membrane surface did not indicate significant antimicrobial properties, the effect of nC_{60} and nAg onto the surface can easily be seen to correlate with high surface concentrations of each particle (Figure 4.7), especially in the case of nAg. Thus, nAg was chosen for future research.

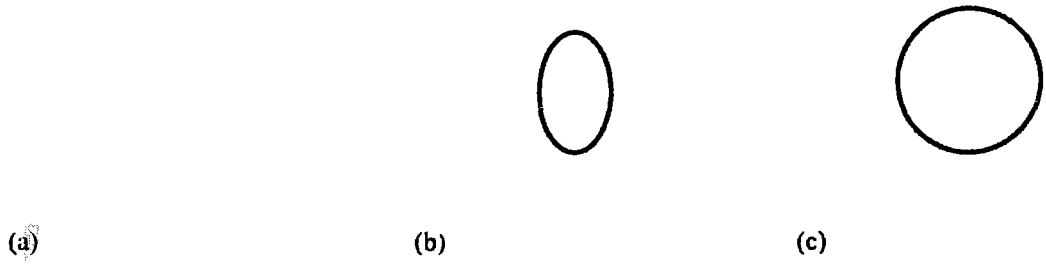

Figure 4.7: Growth of *E. coli* on agar-supported membranes. (a) Commercial polysulfone membrane, (b) polysulfone membrane with 1mg nC_{60} deposited in solution onto the surface with a pipet, (c) polysulfone membrane with 1 mg of nano-Ag deposited in solution onto the surface with a pipet. Patches of no growth (i.e. no tan-colored colonies of *E. coli*) indicate potentially antimicrobial regions of the membrane where a higher concentration of the particles was deposited.

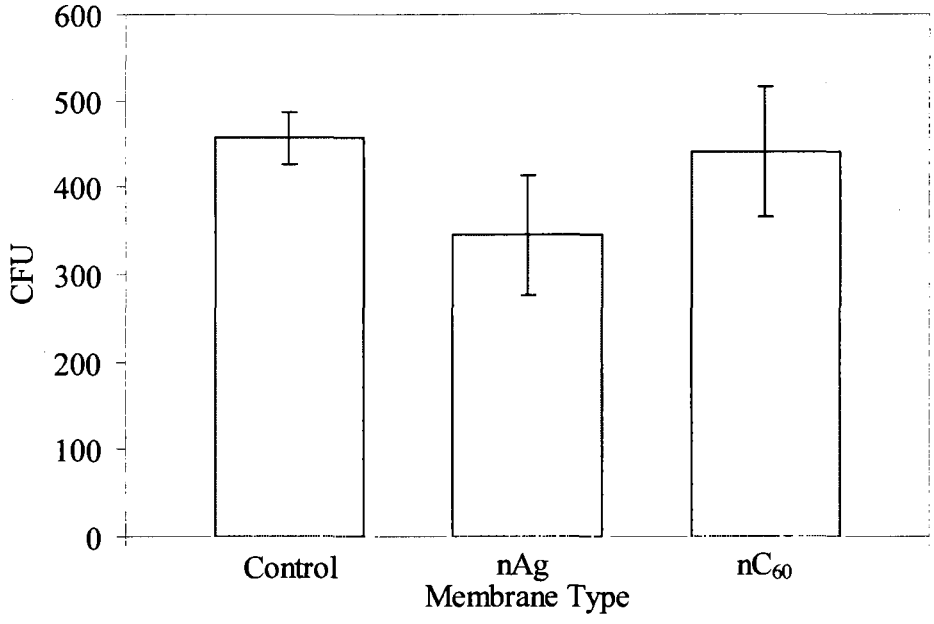

Figure 4.8: Growth of *E. coli* on agar-supported membranes. Commercial polysulfone membranes with nAg and nC_{60} deposited directly on the membrane surface, error bars represent standard deviations. Although local supression of bacterial growth was observed (and pictured in Figure 4.7), the growth of bacteria on the entire membrane surface was not significantly reduced. Membrane disks had an area of 9 cm^2.

5.0 DISCUSSION AND CONCLUSIONS OF PRELIMINARY RESULTS

The potential for nanoparticle incorporation into PSf membranes for biofouling control has been briefly surveyed with respect to some nanoparticles – CNT, carboxylated CNT, C_{60}, PVP/C_{60} and nAg. While the nanotubes, including those with carboxyl functional groups, and nC_{60} incorporated into the membrane matrix by the above procedure showed no antimicrobial effect on the bacterium *E. coli*, membranes with nAg and nC_{60} deposited directly on the membrane surface exhibited some antimicrobial properties. Thus, these two nanoparticles show promise for future research.

These experiments emphasized the importance of bioavailability of nanoparticles to bacteria in membrane biofouling control. Depending on the exact mechanism of toxicity and uptake, it is possible that, although these membranes are effective for a time, their effectiveness will decrease as they are depleted of nanoparticles. The importance of nanoparticle availability with filtration was investigated with nAg and was explained in detail in the main text.

Give the results of this series of experiments, nAg was chosen as the most promising nanoparticle for future research. Its ability to prevent bacterial growth when deposited on a surface has been shown, and experiments to characterize polysulfone membranes impregnated with nAg were conducted.

PART 2:

INCORPORATION OF nAg INTO POLYSULFONE ULTRAFILTRATION MEMBRANES*

*The results and discussion detailed in this section was previously published in: Zodrow, Brunet, Mahendra, Li, Zhang, Li, Alvarez, 2008. Polysulfone ultrafiltration membranes impregnated with silver nanoparticles show improved biofouling resistance and virus removal. Water Res 43, 715-723.

6.0 LITERATURE REVIEW

6.1 Membrane technology for water treatment

The use of membrane technology for water treatment has grown rapidly in the last decade because of their reliability, ease of operation, and compact design (see Figure 6.1). As reliable sources of water grow scarce, membrane technology offers an alternative to conventional water treatment that provides a reliable method for desalination and water reuse. Desalination by reverse osmosis membranes is often a solution for purifying salty or brackish water employed in coastal areas, and water reuse is growing in acceptance around the world. Perhaps the most notable example of a water reuse plant is the Kranji Newater Reclamation Plant in Singapore that uses a dual membrane treatment system and UV disinfection to treat 14.7 million gallons (or 55,600 m^3) water per day (2007). However, two major hurdles remain for low-pressure membrane filtration systems – biofouling and acceptable virus removal. Because they are exposed to either raw water or water treated with a coagulant without sedimentation, membranes are very susceptible to biofouling, which reduces membrane flux and decreases membrane life, and because of their relatively large pores, low-pressure membranes do not remove viruses effectively. These hurdles are areas of constant research.

Membranes separate different components of fluids by selecting for differences in size, shape, or chemical structure. Separation of water constituents across a membrane is performed through the application of a pressure difference across the membrane (called the transmembrane pressure) that facilitates transport of materials across the membrane.

For micro- and ultrafiltration membranes, particles as small as approximately 0.01 μm (such as bacteria and protozoa) are separated from water through size exclusion. Although smaller particles may not be separated this way, they may adsorb onto the membrane surface and thus be retained from the permeate. In non-porous membranes, such as those used for reverse osmosis desalination, water is preferentially transported across the membrane, although no pores are present. Because the pore structure and size and the material of the membrane are controlled to offer the optimal removal efficiency and flow rate, membranes are a very powerful and convenient separation tool. However, increased removal of organisms or compounds through size exclusion is obtained with a costly price – an increase in transmembrane pressure (Figure 6.2). Thus, membrane treatment system designs must compromise between removal efficiency and operation costs.

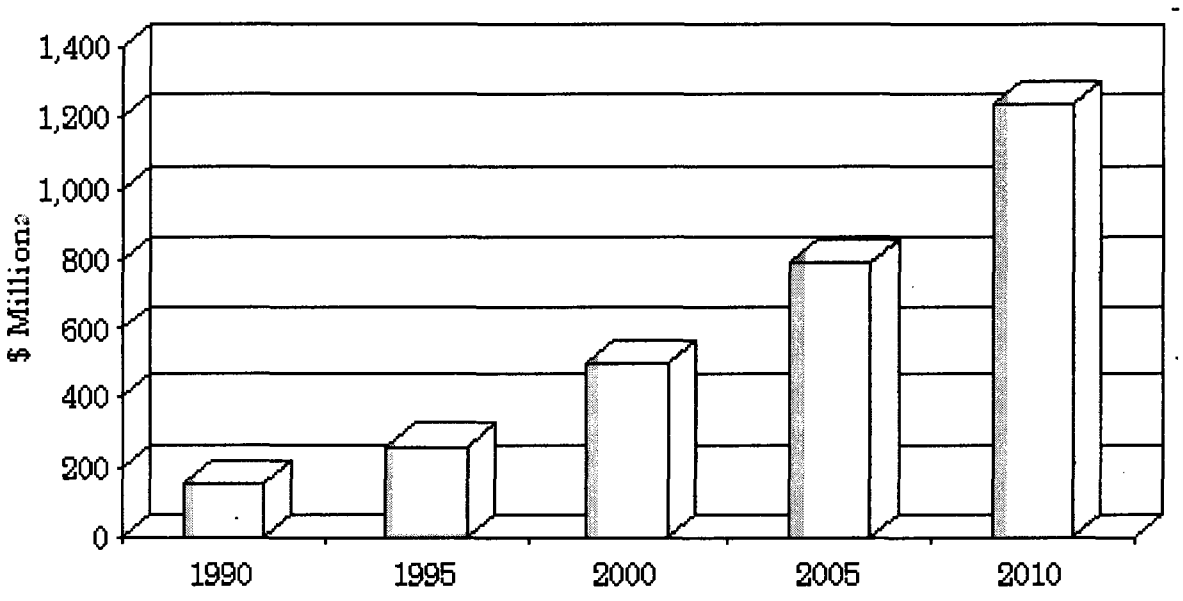

Figure 6.1: Growth of the microfiltration membrane industry (Hanft, 2006)

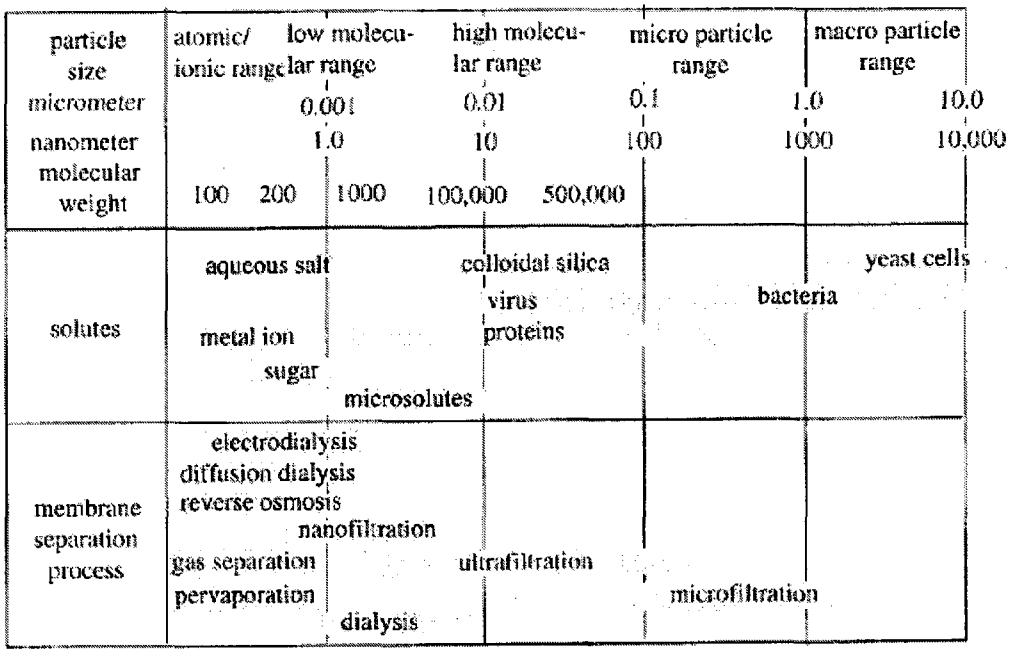

Figure 6.2 Removal of water constituents by different membrane processes (Mulder, 1990).

A variety of membrane configurations are used by the water treatment membrane industry. In general, because of their low cost and high packing density, spiral wound membranes are the most common membrane design for nanofiltration and reverse osmosis systems (Figure 6.3). Hollow fiber membranes (Figure 6.4) are commonly used in micro- and ultrafiltration membrane filtration. These two membrane types offer a compact design and a small water treatment plant footprint (as compared to conventional treatment and other membrane configurations). This quality is particularly appealing to plants that must expand but lack the required space. For example, a water filtration plant in Kennewick, Washington expanded from 7.5 to 16 MGD (28,000 to 56,000 m^3) by installing submerged hollow fiber membranes in the already present granular media basins (2007). Because of their ease of installation, membranes can easily be added to expand existing water treatment plants, used in smaller decentralized systems (as small as individual households), or incorporated into new plants built in areas where land (needed in large quantities in conventional water treatment) is scarce.

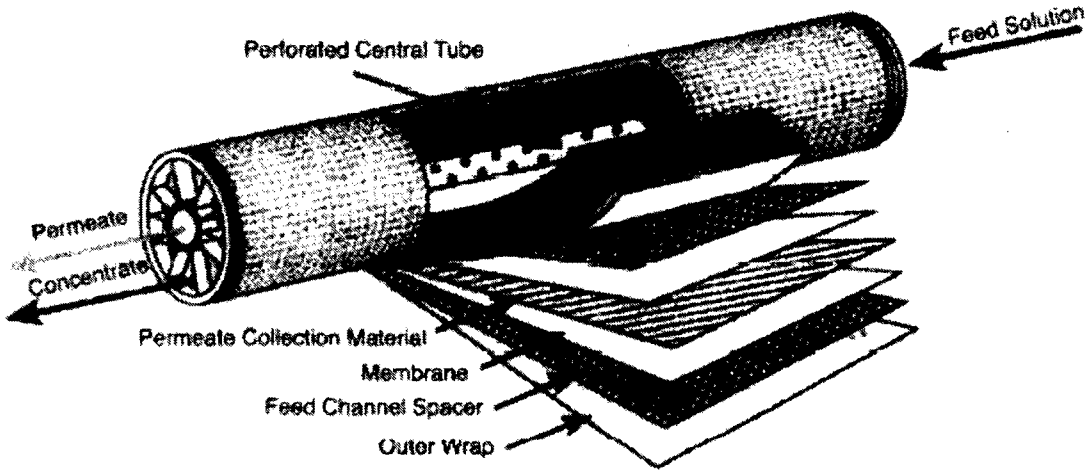

Figure 6.3: Spiral-wound membrane. (Nicolaisen, 2003)

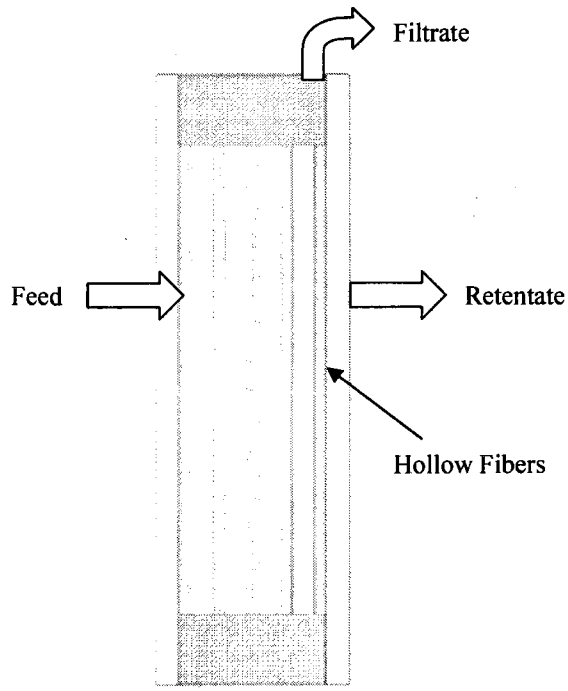

Figure 6.4: Hollow fiber membrane.

6.2 Biofouling of ultrafiltration membranes

Fouling of the membrane is a result of various raw water components, including particles, minerals (such as silica, barium, calcium, and magnesium), microorganisms, and byproducts of microorganism growth. This research focused in part on the prevention of biofouling of water treatment membranes and the associated decrease in membrane flux, increase in energy costs and shortening of membrane life (Mcdonogh et al., 1994).

Biological fouling refers to the formation of a biofilm on the membrane surface. As the biofilm organisms thrive, they secrete extracellular polymeric substances (EPS). These substances are a key component of biological fouling, and the flux decline of a membrane is higher if cells attached to the surface are secreting EPS (Chellam and Xu, 2006; Amy, 2008; Wang et al., 2008). Additionally, although the cake layer of dead cells is easily removed and clean membrane flux is nearly restored with a membrane backwash procedure (where flow through the membrane is reversed), clean membrane flux will not be restored after bacteria on the surface produce a large amount EPS (Chellam and Xu, 2006). Thus, membranes must be backwashed frequently to prevent the buildup of EPS and irreversible fouling.

Membrane biofouling is commonly controlled with pretreatment (coagulation), backwash procedures, chemical cleaning (e.g., chlorine), or through the control of membrane and operational parameters. Although coagulation is commonly used in conventional water treatment, it is likely that optimal coagulant doses for membrane filtration are different from those commonly used in conventional treatment. The commonly acidic conditions during coagulation in conventional water treatment produces small flocs that can enter the pores of the membrane and cause irreversible fouling

(Kimura et al., 2008). Thus, proper coagulant types and dosages for microfiltration biofouling prevention are an area of ongoing research. In addition to water pretreatment, biofouling is often controlled through the use of chlorine during the backwash procedure. However, many polymeric membranes cannot withstand the corrosiveness of these chemical cleaners, and the formation of disinfection byproducts (DBP) in drinking water treatment, especially in the highly organic backwash waste stream, is an ever-growing concern. Additionally, chemicals are expensive, and the presence of large amounts of chlorine in water treatment plants is a growing safety concern. Membrane biofouling may also be reduced by operation at very high temperatures. For example, reverse osmosis membranes made by Duratherm™ can withstand temperatures as high as 90°C (Nicolaisen, 2003). However, operation at these high temperatures increases energy costs and decreases solute rejection, decreasing operating efficiency. Because pretreatment, chemical cleaning, and membrane operation control of biofouling all have significant drawbacks, other methods of biofouling reduction have been explored.

Certain membrane characteristics affect the likelihood of cell attachment, including surface charge and hydrophobicity (Ridgway et al., 1999). Because many of the components in raw water that have the potential to foul the membrane are negatively charged and hydrophobic, membranes that are more negatively charged and hydrophilic will foul less. The membrane surface morphology also plays a significant role in membrane fouling reduction. Increasing the smoothness of the membrane decreases the available surface area for microbial and particle attachment and thus decreases the likelihood of biological fouling (Vrijenhoek et al., 2001). Therefore, the chemical and

surface characteristics of a membrane are commonly controlled in order to reduce the membrane's fouling potential.

6.3 Virus removal using ultrafiltration membranes

According to the Surface Water Treatment Rule (SWTR), a water treatment process must be designed to provide a 4-log (99.99%) removal or inactivation of viruses (2007). The use of microfiltration and ultrafiltration to remove viruses from water and wastewater is limited by the small size of viruses compared to the relatively large pore size of the membranes (Zhu et al., 2005). Also, membrane surface imperfections can increase the possibility of virus penetration during filtration (Bellara et al., 1998). Although some ultrafiltration membranes effectively remove viruses (Lovins et al., 2002), polymeric microfiltration and ultrafiltration membranes do not always experience effective virus removal without particular pretreatment or post-treatment procedures. The exact reason for these differences in removal by ultrafiltration membrane is somewhat unclear, but it may be directly related to the transmembrane pressure; i.e., systems operated at a higher transmembrane pressure experience lower virus removal rates (Arkhangelsky and Gitis, 2008). Regardless, additional methods of virus removal in low-pressure membrane systems would benefit the water treatment industry.

Two effective methods for increasing virus removal efficiency in water treatment include coagulation with metal salts (Zhu et al., 2005) and inactivation with chlorine, ozone, and ultraviolet light (Thurston-Enriqueza et al., 2005). A 4-log removal of MS2 can be obtained at pH 6.3 with the addition of 10-mg/L Fe coagulant (Zhu et al., 2005). This required virus inactivation is reliably obtained by 0.60 mg/L/min of ozone at 5°C

and pH 7 for adenovirus type 40 and 0.03 mg/L/min ozone for feline calicivirus (Thurston-Enriqueza et al., 2005). Although UV effectively inactivates bacteria and some protozoa, it is ineffective against some viruses, including MS2 (Butkus et al., 2005; Kim et al., 2008). Two particular problems arise with the effective virus removal methods. When viruses are coagulated with metal salts, they are incorporated into the settled flocs; they are not inactivated (Zhu et al., 2005). Thus, the viruses incorporated into flocs will later be incorporated into fertilizers used on agricultural fields. Although ozone and UV can both be used to inactivate many viruses (along with acting as disinfectants towards other microorganisms and potentially inducing oxidation of other organics), they are potentially expensive and energy-intensive processes. Also, the use of chlorine for disinfection of viruses leads to the formation of harmful DBPs. Thus, a need exists for effective and inexpensive virus removal during membrane filtration.

6.4 Antibacterial and antiviral properties of silver nanoparticles and ions

For millennia people have taken advantage of the antimicrobial properties of silver, employing methods as simple as storing drinking water and milk in silver containers and as complex as silver-coating medical implants and instruments (Davies and Etris, 1997; Bosetti et al., 2002; Li et al., 2008). The lower thresholds for silver ion (Ag^+) toxicity lie between 0.01 and 0.1 mg/L (Ratte, 1999; Cunningham et al., 2008), while the World Health Organization established a secondary standard of 0.1 mg/L of silver in drinking water. This standard allows for a total dose over 70 years of one-half of the human no observable adverse effect level (NOAEL) of 10 g to prevent argyria, a disease associated with a silver coloring of the skin (WHO, 2004). In humans, silver ions cannot cross the

blood-brain barrier, and they are regulated by blood metallothioneins, which bind silver ions in metal-thiolate-cluster structures for transport, storage, and detoxification (Davies and Etris, 1997). Perhaps the most significant difference between humans and bacteria and viruses and the reason silver ions are considered for water disinfection is a lack of thiol groups, directly related to silver inactivation of bacteria, on mammalian cell surfaces (Ratte, 1999).

The antibacterial mechanism of silver is related to its interaction with sulfur and phosphorus, most notably thiol groups (S-H) present in cysteine and other biochemical compounds (Davies and Etris, 1997). Interaction of ionic silver (which can be released from nAg) with thiol groups and formation of S-Ag or disulfide bonds can damage bacterial proteins, interrupt the electron transport chain, and dimerize DNA (Trevors, 1987; Russell and Hugo, 1994; Feng et al., 2000). Cells treated with non-lethal levels of silver ions show DNA aggregation in the cell (Feng et al., 2000), and cells that have been damaged by silver ions can be repaired with cysteine (Russell and Hugo, 1994).

Silver nanoparticles may damage some bacteria and viruses by mechanisms other than the release of silver ions. Silver ion dissociation from nAg can account for approximately 1% of the total silver present (Navarro et al., 2008). Thus, the full toxicity of nAg cannot be explained solely by the release of silver ions – the nanoparticles themselves exhibit some mechanism for toxicity (Navarro et al., 2008). It may be that the oxidative stress on the cell surface caused by nAg or the creation of reactive oxygen species, ROS, is the main cause of nAg particle toxicity (Hwang et al., 2008). In other studies, damage to the cell wall of nAg-exposed bacteria was visually apparent, and cell death was suspected to be due to an increase in cell membrane permeability that lead to

osmotic collapse and a release of intracellular material (Sondi and Salopek-Sondi, 2004; Morones et al., 2005; Panacek et al., 2006). The toxicity of nAg to bacteria is greatly influenced by nAg particle size and shape. While nAg synthesis and uptake in bacteria has been reported for spheres and rods up to 80 nm (Pal et al., 2007), particles in the range of 1 to 10 nm with high density <111> facets are most likely to interact negatively with the cell (Xu et al., 2004; Morones et al., 2005; Gogoi et al., 2006; Pal et al., 2007). The toxicity mechanisms of Ag^+ ions that dissolve from nAg are well understood, but the extent to which direct contact between bacteria and nAg causes toxicity remains unclear.

The antiviral properties of silver ions may involve interaction with viral DNA and thiol groups in proteins (Russell and Hugo, 1994). Silver ions have been shown to be effective antiviral agents towards MS2 (Yahya et al., 1992; Kim et al., 2008), a common indicator of enteroviruses used in water treatment models (Zhu et al., 2005). Although virus inactivation rates for Ag^+ are slower than those for free chlorine ($10^{0.013}$/min for 40 μg/L Ag^+ vs. $10^{3.35}$/min for 0.2 μg/L free chlorine), the inactivation rate may be enhanced through the use of UV light (Yahya et al., 1992; Zhu et al., 2005). Thus, Ag^+/UV may be used for virus inactivation as a chlorine alternative. Silver nanoparticles are effective at inactivation of Monkeypox Virus (similar clinically to smallpox) (Rogers et al., 2008) and HIV-1 (Elechiguerra et al., 2005). Although the exact mechanism of nAg inactivation of monkeypox is unknown, HIV-1 viruses were inhibited from binding to host cells by nAg particles ranging from 1-10 nm that preferentially bound to viral gp120 glycoproteins (Elechiguerra et al., 2005). Thus, the incorporation of nAg into water filtration membranes shows promise as both nAg and Ag^+ act as antiviral agents.

6.5 *Use of nanomaterials in water treatment*

The use of nanomaterials in water treatment is extensively studied at the lab scale. In addition to nanoparticle addition to water filtration membranes, titanium dioxide nanoparticles (TiO_2), carbon nanotubes (CNT), fullerol, and magnetite are studied for their catalytic, sportive, and permeable properties.

TiO_2 and fullerol are photocatalysts and can be used in a batch system or in conjunction with a membrane or surface to degrade organics and inactivate bacteria (Oka et al., 2008). TiO_2 may also be fixed to a surface to better utilize its photocatalytic properties (Xu et al., 2008).

Carbon nanomaterials, such as C_{60} and CNT have been explored as potential membrane additives. C_{60} was added to membranes for the catalytic destruction of estrogenic compounds (Polotskaya et al., 2007). Additionally, CNT deposited onto a surface have been shown to inactivate *E. coli* through puncturing of the cell membrane (Kang et al., 2008). Carbon nanotubes can be aligned to produce a very hydrophobic high flux membrane. This membrane can be engineered for a very specific pore size. The idea of aligning CNT for use as a filter began with Jirage et al. and was later expanded by many others (Jirage et al., 1998; Mauter and Elimelech, 2008). Membranes made out of aligned CNT have flow rates of 4-5 orders of magnitude higher than those predicted by fluid mechanics, possibly due to the high hydrophobicity of the nanotube channels and the molecular alignment of water molecules as they flow through the channels. These properties cause the flow to violate the no-slip boundary condition (Mauter and Elimelech, 2008). The use of nanoparticles as sorbents in water filtration is also great, and magnetite has been shown to effectively remove arsenic and other heavy

metals (Yavuz et al., 2006). Thus, the potential for nanomaterials use in water treatment is great, and the use of nanomaterials may increase the efficiency and effectiveness of water treatment over conventional processes.

6.6 Silver nanoparticles in water treatment membranes

Incorporation of antimicrobial nanomaterials into membranes offer an innovative potential solution to biofouling control (Savage and Diallo, 2005; de Prijck et al., 2007; Li et al., 2008), and silver ions and nAg have been studied for a wide variety of water treatment processes, including water filtration membranes. Nanosilver has been incorporated into cellulose acetate (Chou et al., 2005), polyimide (Deng et al., 2008), polyamide (Damm et al., 2007), and poly(2-ethyl-2-oxazoline (Kang et al., 2006) membranes on the lab scale. However, the long-term effectiveness of the incorporated nAg in preventing biofouling during continuous filtration has not been addressed. Furthermore, little research has been conducted on the incorporation of nAg in polysulfone membranes, which are notable for their widespread application in water filtration (in microfiltration, ultrafiltration, and occasionally, nanofiltration membranes). This motivated the experiments presented herein, which address the antimicrobial and antiviral properties of polysulfone membranes impregnated with nAg and their application for biofouling and virus control.

7. 0 MATERIALS AND METHODS

7.1 Membrane fabrication

Polysulfone ultrafiltration membranes were made using the wet phase-inversion process (Mulder, 1990). First, poly(vinyl pyrrolidone) (PVP, MW: 55,000; Sigma-Aldrich) was dissolved in the solvent *N*-methyl-2-pyrrolidone (NMP, 99.5%; Sigma-Aldrich) at 50°C with stirring. Silver nanoparticles (1-70 nm; Novacentrix, Austin, Texas) were added and dispersed in the solvent with a sonicating probe (Fisher Scientific Sonic Dismembrator Model 100). The solution was heated to 120°C, and polysulfone (PSf, Udel P3500; Solvay Membranes) was added. The final solution was composed of 15% PSf, 10% PVP, 75% NMP, and (in the nAg-PSf membrane) 0.22% nAg by weight. After the solution was cooled, a thin film of the casting solution was deposited onto a glass plate using an aluminum casting knife. The glass plate and membrane film were quickly transferred to a water bath at room temperature for the remainder of the phase inversion process.

7.2 Membrane characterization

Membrane permeability was determined from clean water flux measurement using deionized water at room temperature and a Sterlitech dead-end filtration cell over a pressure range of 0.34 to 14 bars. Before the permeability measurement, the membrane was compacted at a pressure of 14 bars. Hydrophobicity of the membranes was determined by sessile drop contact angle measurement of water on membranes that were dried overnight (DROPImage Standard). Membrane surface zeta potential was measured

to determine whether incorporation of nAg changes membrane surface charge. Streaming potential measurement was conducted in a 10^{-2} M NaCl background solution (a concentration similar to that used in bacterial experiments) at pH 5, 7, and 9 (ZetaCAD, CAD Instrumentation; Les Essarts Le Roi, France) (Fievet et al., 2003). Images of dried membrane cross-sections were taken with a scanning electron microscope (FEI Quanta 400 ESEM FEG, 20 kV) in high vacuum mode after coating with approximately 10 nm of gold (CrC-150 Sputtering System, TORR International) to observe membrane asymmetry and pore structure. To measure silver content, the membrane was digested by sonication in 2% HNO_3 (Branson Ultrasonic 5510; Danbury, CT) for 3 days. After digestion, the suspension was filtered through a 1 μm-pore-size glass fiber filter (Gelman, Type E) to remove large particles, and analyzed for total silver content. Total silver recovery by this method was 104% ± 0.3% (n = 3).

Total silver concentrations were quantified using a Perkin-Elmer Optima 4300 DV Inductively Coupled Plasma-Optical Emission Spectrometer, ICP-OES (Norwalk, CT). All measurements were carried out in the axial mode at 328.068 nm. Yttrium (371.029 nm) was used as an internal standard for calibration as recommended by the ICP manufacturer. All samples and ICP standards were acidified by 0.5% trace metal grade HNO_3. The detection limit of silver for the ICP was 0.01 mg/L.

Analysis of silver present on the surface of the membrane was conducted using X-Ray Photoelectron Spectroscopy (PHI Quantera XPS). Volumes of 1 and 4 L of deionized (DI) water were filtered through nAg-PSf membranes with a vacuum filtration cell. The membranes were dried thoroughly before analysis. A detailed scan for silver was conducted at a range of 362 to 385 eV.

7.3 Analysis of silver in the filtrate

Four liters of deionized (DI) water were filtered with a vacuum filtration cell, and the total silver concentrations in the filtrate were quantified using ICP as described above. Silver leaching mainly in ionic form was confirmed by TEM analysis (JEM FasTEM 2010; 200 kV accelerating voltage), as the mass of silver recovered in nanoparticle form accounted for less than 10^{-7} percent of the silver in the filtrate. For this analysis, five drops of filtrate (5 µL) were placed on a carbon grid (Type A, 300 mesh; Ted Pella, Inc.; Redding, CA, USA). Each drop was allowed to dry thoroughly before the next drop was applied. For the mass balance, it was assumed that the density of nAg was equivalent to that of metallic silver (i.e., 10.5 g/cm^3) (Kaye and Laby, 1986). The size and number of silver particles was determined with ImageJ (National Institute of Health).

7.4 Antibacterial properties of nAg-PSf membranes

To assess initial effectiveness of the antibacterial properties of the membranes, 3 mL of stationary phase *Escherichia coli* K12 (American Type Culture Collection, ATCC, 25404) was serially diluted to 10 CFU/mL from a stock of 10^9 CFU/mL (OD_{600} 1 – 1.5, measured by Ultrospec 2100 Pro, Amersham Biosciences) in Minimal Davis (MD) medium (0.7 g/L K_2HPO_4, 0.2 g/L KH_2PO_4, 1 g/L $(NH_4)_2SO_4$, 0.5 g/L Na-citrate, 0.1 g/L $MgSO_4 \cdot 7H_2O$) and was filtered onto sterile PSf and nAg-PSf membranes using a vacuum filtration cell (both the membranes and the filtration cell were previously autoclaved at 121°C for 15 minutes). Membranes were then placed on Luria-Bertani (LB) agar plates and incubated at 35°C overnight. Colony forming units (CFU) on the membrane surface

were counted on the following day, giving the total number of viable cells after filtration and incubation.

The antibacterial contribution from silver contained in the membrane was evaluated with the use of the amino acid cysteine (Sigma; St. Louis, Missouri, USA). Cysteine forms complexes with Ag^+ released from nAg, making Ag^+ ions unavailable to act as antimicrobial agents (Silver and Phung, 1996; Liau et al., 1997; Navarro et al., 2008). However, full discernment of the antibacterial role of Ag^+ may not be possible with this approach because cysteine may also bind to nAg particles and reduce their bioavailability (Santos et al., 2007), which confounds the interpretation of decreased toxicity attributable solely to Ag^+ complexation. Batch growth experiments were performed with *E. coli* K12 in MD with 1 g/L glucose in the presence of cysteine. After two hours of incubation, the suspension was spiked with 2.7 mg/L nAg. The optical density at 600 nm was monitored (Ultrospec 2100 Pro, Amersham Biosciences) as an indicator of bacterial growth.

7.5 Biofouling resistance of nAg-PSf membranes

The attachment of bacteria to the membrane surface was assessed with *E. coli* in MD medium. Stationary phase bacteria (~10^9 CFU/mL) were incubated with 1-cm^2 PSf and nAg-PSf membrane coupons at 35°C while shaking for 4 h. This incubation time resulted in a visible layer of attached bacteria with low enough cell colony density to remain countable. The membranes were removed from the media and rinsed gently with sterile deionized water thrice. Bacteria on the membrane, specifically the nucleic acids, were stained with 1 μg/mL 4',6-diamidina-2-phenylidole (DAPI) for 5 minutes and then

rinsed. Membrane coupons were mounted to a glass slide and viewed with a fluorescence microscope (Zeiss Axioplan, MetaMorph Software). DAPI showed little background fluorescence on membranes that had not been exposed to bacteria. Cells were enumerated with the software ImageJ (National Institute of Health) and cell density on the membrane was calculated.

The potential of biofilm formation on the membrane surface was evaluated using the method described by de Prijck et al. (2007). Briefly, stationary phase cultures of *Pseudomonas mendocina* KR1, a prolific biofilm forming bacterium (Jayasekara et al., 1999), were diluted to OD_{600} 10^{-6} (10^3 cells/mL) and incubated with a sterile membrane coupon (PSf and nAg-PSf) in 5 mL of MD media for 24, 48, and 72 hours. Both the planktonic cells in the supernatant and the sessile cells in the biofilm were counted. To enumerate the planktonic cells, three to five-fold dilutions were plated onto LB agar plates and incubated overnight. Colony forming units (CFU) were counted the following day. To measure the number of cells attached to the membrane, the membranes were removed from the media and rinsed with sterile DI water. The membranes were placed in 2 mL of fresh MD media, vortexed (Vortex Genie 2, VWR Scientific) on the highest setting for 30 seconds and placed in a sonication bath for 30 seconds. This biofilm disruption procedure was performed twice. Samples were taken directly from the supernatant, deposited on a LB agar plate, and incubated overnight. The CFU on the plates were then counted. The influence of cysteine (used as Ag^+ ligand) on biofilm growth on the nAg-PSf membrane was measured similarly, but in the presence of 27 mg/L cysteine. This concentration was chosen to assure a surplus of cysteine to chelate silver present in the membrane. In order to examine the effectiveness of nAg

impregnation to control of silver-resistant bacteria, biofouling experiments were repeated with *Pseudomonas aeruginosa* (ATCC 700829) harboring metal resistance *czc* genes (Hassen et al., 2001), with an initial concentration of 10^7 cells/mL.

7.6 Virus removal by nAg-PSf membranes

The bacteriophage MS2 (ATCC 15597-B1) was used in this study. MS2 is a single-stranded RNA virus that is commonly used as an indicator for enteric viruses and is similar in size, shape, and nucleic acid content to common human pathogens, including the hepatitis A virus and poliovirus (Zhu et al., 2005). Additionally, because MS2 is one of the smaller viruses, it can often act as a worst-case scenario for membrane filtration (Zhu et al., 2005). Bacteriophage MS2 was propagated according to a previously published method (Zhu et al., 2005) with minor modifications. Initial concentrations of MS2 phage in the range of 10^4 to 10^5 plaque-forming units per milliliter (PFU/mL) suspended in 2 mL 0.1 M bicarbonate buffer were filtered through the nAg-PSf and control PSf membranes. Virus concentrations were assayed using an agar-overlay technique (Kennedy et al., 1986). Briefly, 100 μL aliquots of influent or filtrate were serially diluted in 900 μL bicarbonate buffer, and incubated with 100 μL stationary phase MS2 host *E. coli* (ATCC 15597) for 10 minutes. This mixture was added to 3 mL warm (45°C) tryptic soy soft agar, overlaid upon Luria-Bertani agar plates, and incubated at 37°C. Plaques were counted after 24 hours, and removal was calculated as logarithm of the ratio of PFUs in the filtrate to those in the influent.

8.0 RESULTS AND DISCUSSION

8.1 Membrane characterization

Membranes impregnated with 0.9% (by weight) nAg (nAg-PSf) had similar permeability and surface charge to the control membrane without nAg (PSf) (Table 8.1). The permeability of both membranes was typical of ultrafiltration membranes (Cheryan, 1998). The nAg membrane was significantly more hydrophilic than the control ($p < 0.05$), with a contact angle 10% smaller than that of the PSf membrane. This decrease in hydrophobicity can be potentially beneficial in preventing chemical fouling, but is beyond the scope of this study and will not be discussed here. Cross-section images of the membrane showed very similar morphologies. The asymmetry of the membrane was apparent and the addition of nAg to the membrane did not visibly alter the membrane structure (Figure 8.1).

Table 8.1: PSf and nAg-PSf membrane properties. The values are represented as average and standard deviation.

	PSf	**nAg-PSf**
Permeability ($L/m^2/h/bar$)	408 ± 180	532 ± 117
Zeta Potential at pH 7 (mV)	-6.5 ± 1.1	-6.9 ± 0.3
Hydrophobicity (Contact Angle, °)	76.8 ± 4.83	68.6 ± 6.1*
Thickness (mm)	0.116 ± 0.0134	0.096 ± 0.0137*

* Denotes significant difference at the 95% confidence interval.

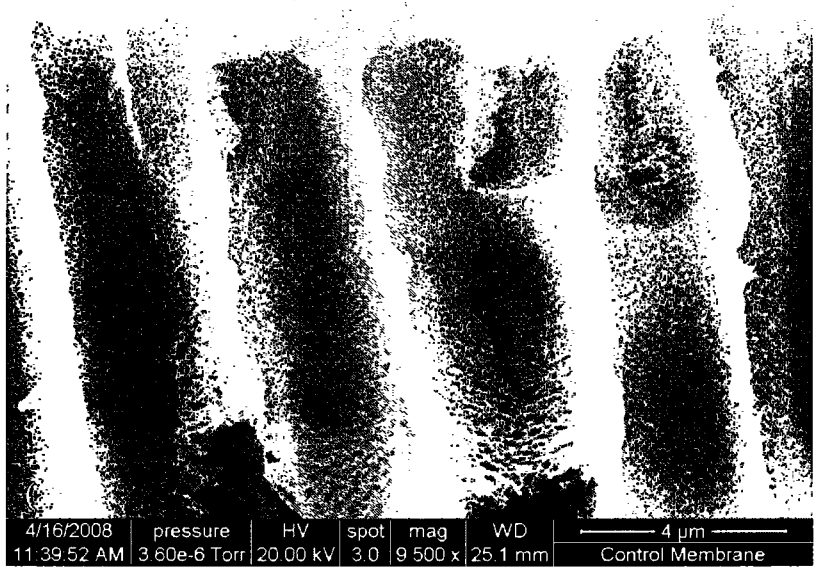

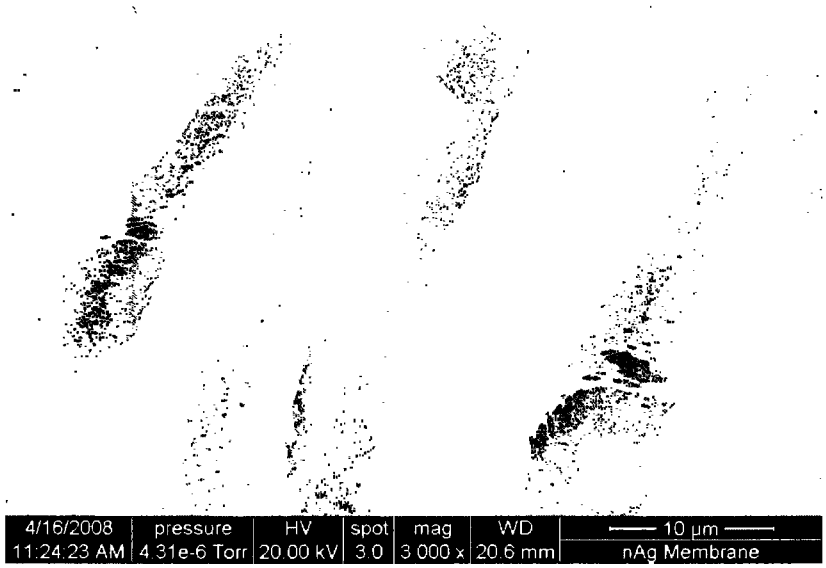

Figure 8.1: Cross sections of membranes. PSf (a) and nAg-PSf (b) membranes taken with SEM. The addition of nAg does not change basic membrane morphology.

8.2 Analysis of silver in the filtrate

The leaching of Ag^+ was confirmed by ICP and TEM analyses. Concentrations of silver as high as 0.034 mg/L were found in the membrane permeate that was filtered at a rate of 0.004 $mL/cm^2/s$. The silver concentration in the filtrate decreased as more water was filtered, and after approximately 0.31 L/cm^2 of filtration, no more silver was detected in the filtrate. TEM analysis of a concentrated solution of the filtrate revealed that the silver leached from the membrane was predominantly in ionic form. Although a few nAg particles were observed in the filtrate, these particles accounted for less than 10^{-7} percent of the total silver concentration of the filtrate. XPS analysis of the membrane indicated that silver was nearly depleted from the membrane surface after 0.4 L/cm^2 of filtration (Figure 8.2), even though ICP analysis of the digested membrane indicated that 90% of the added silver remained within the membrane (Figure 8.3). Thus, the 10% Ag loss was mostly from the surface, the most likely location for membrane-bacteria and membrane-virus interactions. The antimicrobial and anti-viral properties of the nAg membrane were greatly reduced after leaching of Ag^+ stopped even though 90% of the added nAg remained in the membrane (Figure 8.4 & Table 8.2). These results suggest that Ag^+ was the main antimicrobial agent.

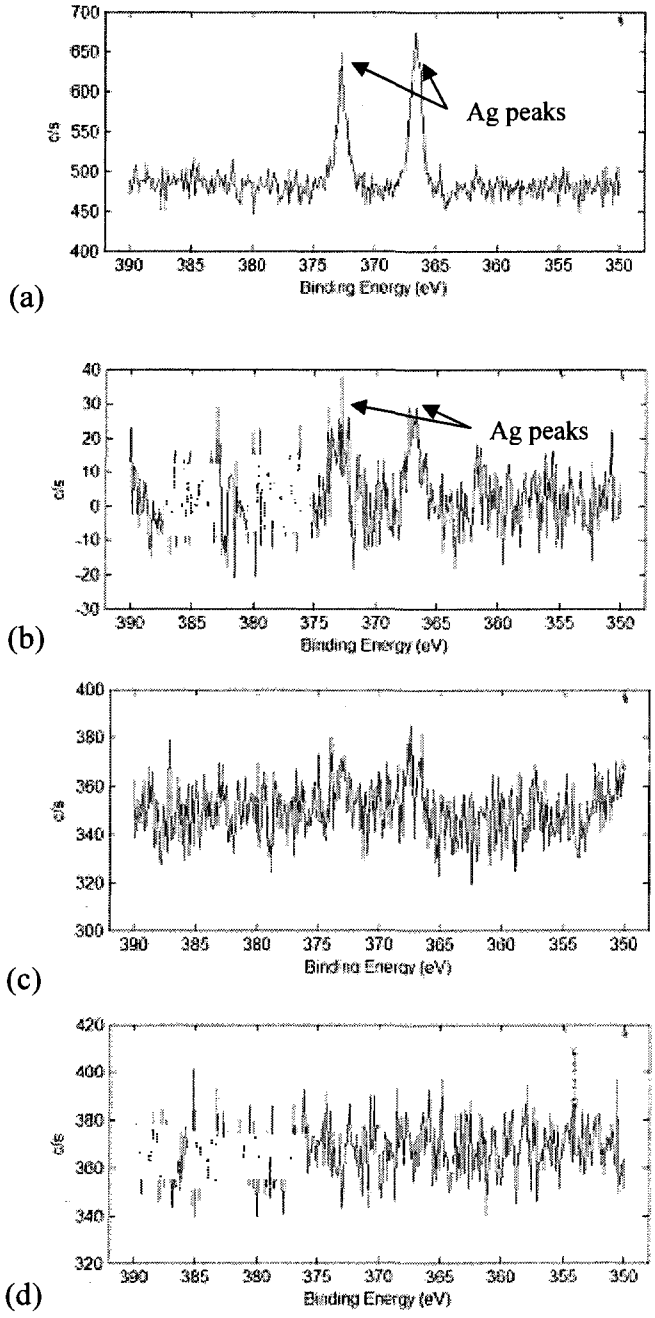

Figure 8.2: Silver detected on surface of membrane with XPS on fresh nAg-PSf membrane (a), a nAg-PSf membrane after 1 L of DI water was filtered (b), nAg-PSf membrane after 4 L of DI water was filtered (c), and the control membrane (d). The distinct loss in silver-related peak corresponds to a loss of silver from the membrane with filtration (Zodrow et al., 2009).

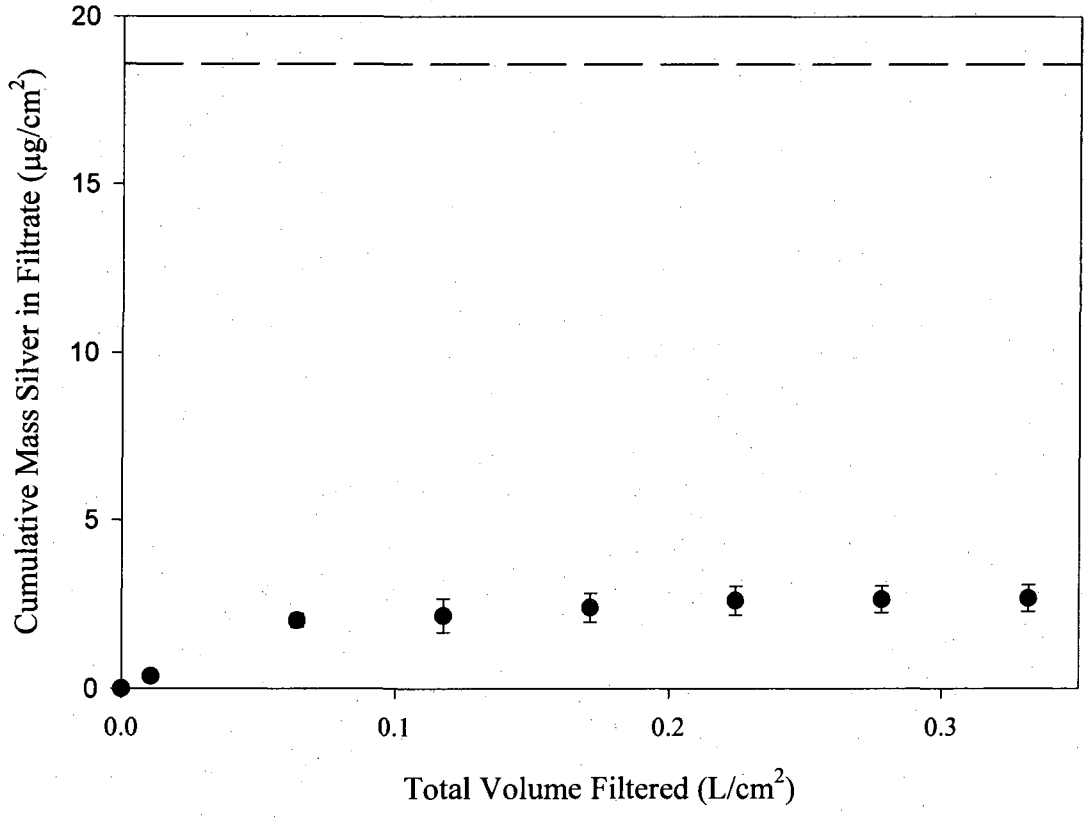

Figure 8.3: Cumulative mass of silver lost from membrane with dead-end filtration of DI water. No silver is detected in filtrate with ICP after 0.3 L/cm^2 of water was filtered. The membrane loses about 10% of total silver (Zodrow et al., 2009).

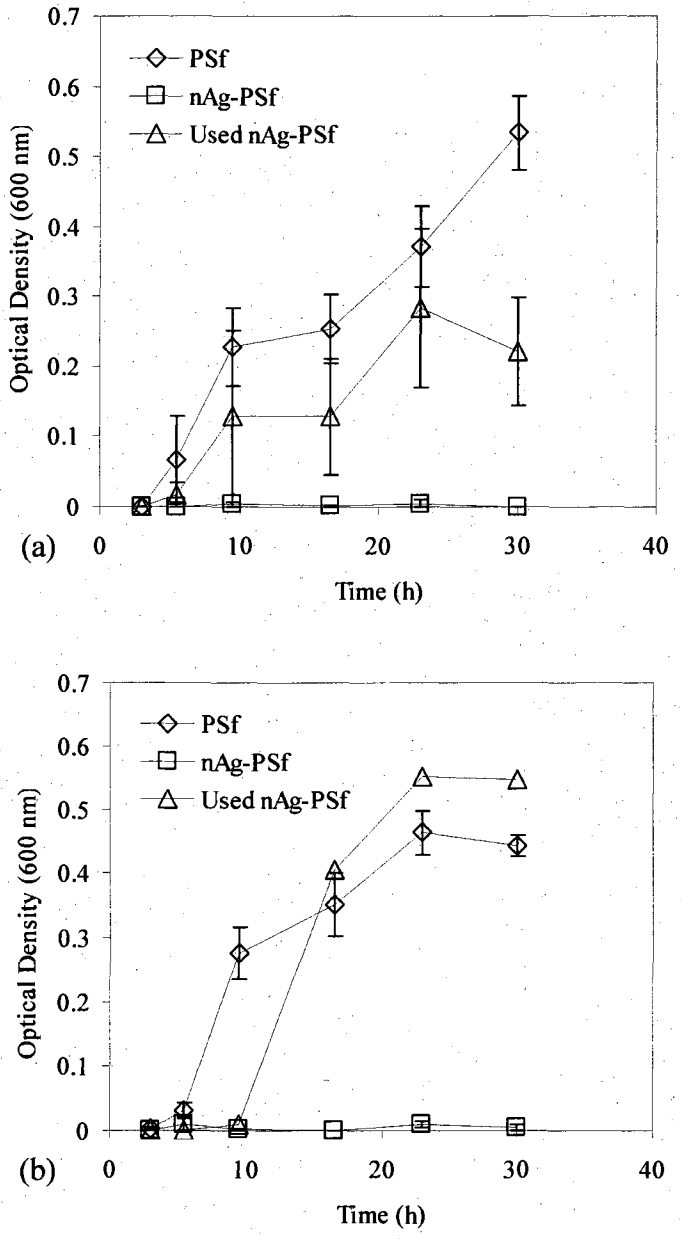

Figure 8.4: The used nAg-PSf membrane was ineffective against *E. coli* (a) and *P. mendocina* (b). Here the OD_{600} was measured in the supernatant of a bacterial suspension incubated at 35°C with a 1-cm^2 membrane coupon. The initial OD_{600} was 0.001 and the initial volume of MD medium was 2 mL with 1 g/L glucose. Error bars indicate results range.

Table 8.2: Viruses removal was not enhanced during filtration by used nAg-PSf membranes. The values are expressed as average and standard deviation (n=4).

Influent (PFU/mL)	Filtrate PSf (PFU/mL)	Filtrate nAg-PSf (PFU/mL)
$4 \pm 2 \times 10^6$	$3 \pm 1 \times 10^6$	$2.9 \pm 1 \times 10^6$

8.3 Antimicrobial properties of membranes

When a suspension of *E. coli* was filtered onto a nanosilver-containing membrane (nAg-PSf) with a dead-end filtration cell, a 2-log (99%) reduction in *E. coli* grown on the membrane surface was observed (Figure 8.5a). Apparently, silver was initially bioavailable at concentrations sufficient for *E. coli* and inactivation. Fluorescent microscopy also showed that the incorporated nAg reduced the attachment of an *E. coli* suspension to the surface of the immersed membrane coupons by 94% (Figure 8.5b), most likely due to a decrease in cell viability. This significant decrease in bacteria attachment was visually apparent (Figure 8.6). These two experiments infer that nAg-PSf membranes exhibit potent antimicrobial properties and are resistant to biofouling, as *E. coli* was inactivated when deposited onto the membrane surface and was less likely to attach when the membrane is exposed to a suspension of cells.

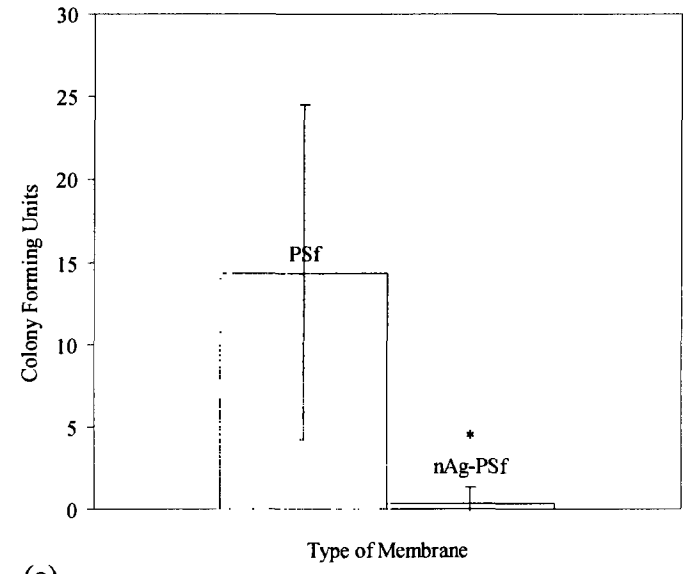

(a)

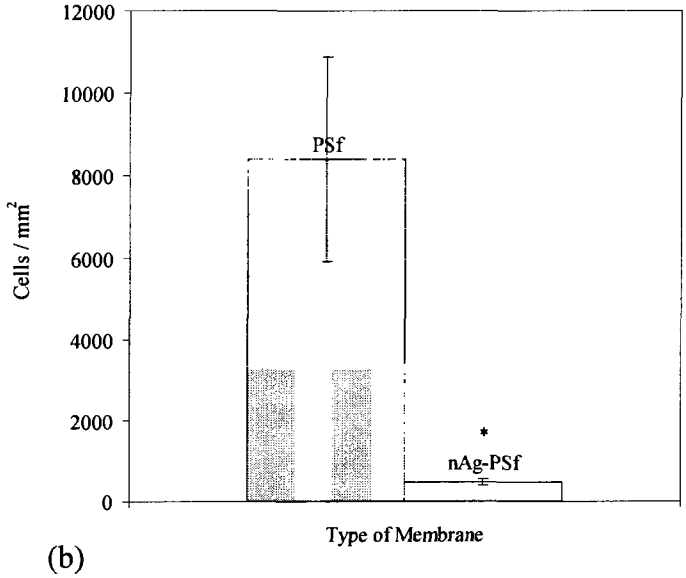

(b)

Figure 8.5: Antibacterial properties of nAg-PSf membrane. Panel (a) shows the number of viable *E. coli* on membrane surface after filtration of 3 mL of bacteria diluted to OD_{600} 10^{-8}, as indicated by the number of colony forming units. Panel (b) shows the number of *E. coli* attached to membrane surface after 4 hours of incubation in MD medium. Error bars indicate 95% confidence intervals (Zodrow et al., 2009).

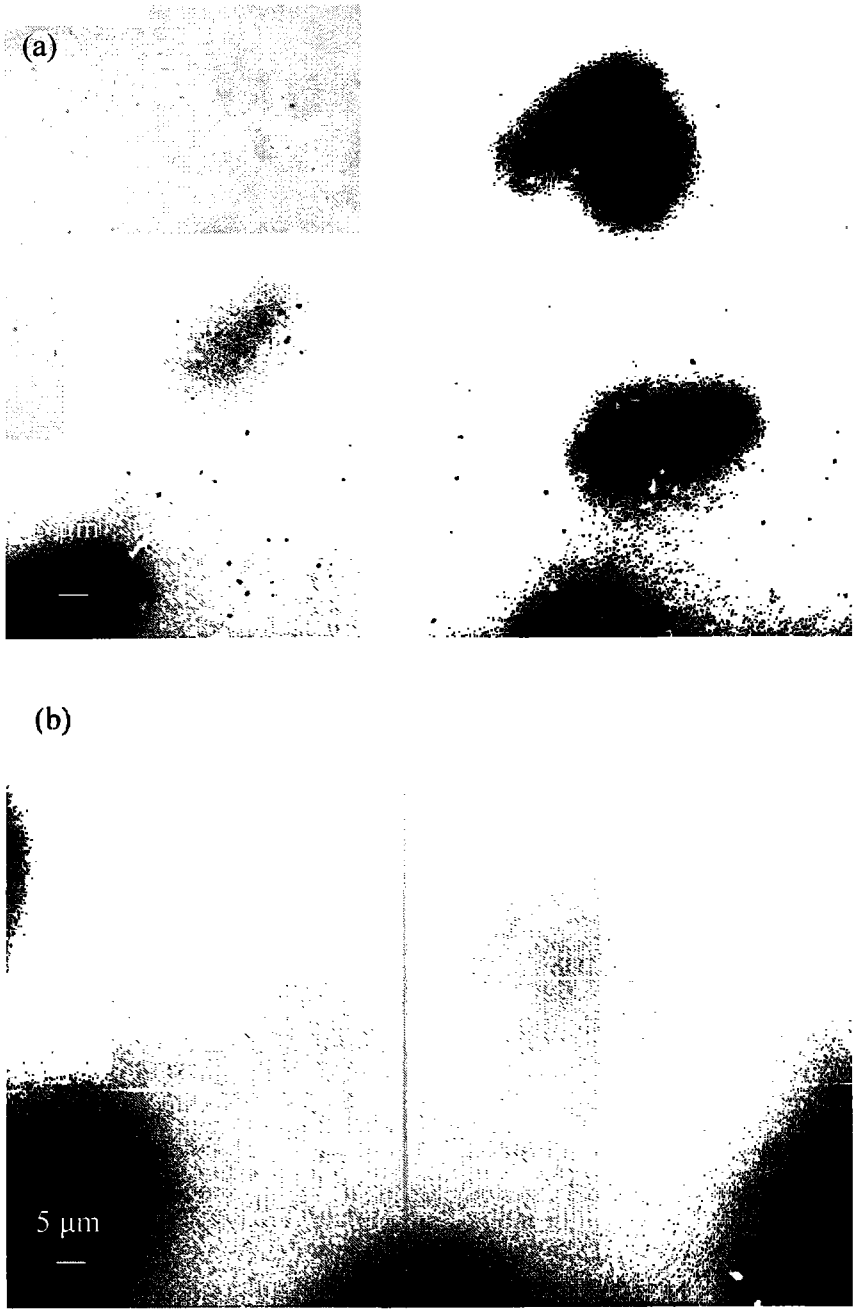

Figure 8.6: Attachment of *E. coli* to membrane surface on (a) PSf and (b) nAg-PSf membranes. Cells were stained with DAPI and viewed with a fluorescence microscope.

8.4 Biofouling resistance of nAg-PSf membranes

When biofilm formation was assessed using *P. mendocina*, very little growth (if any) was observed on the nAg-membrane or in the solution surrounding the membrane (Table 8.3). This antimicrobial activity was attributed mainly to Ag^+ released from the membrane (see analysis of silver in the filtrate, below). Specifically, cysteine was used to bind Ag^+ and restrict its bioavailability required for killing bacteria (Figure 8.7). While no growth of *E. coli* was observed in the presence of a 2.7 mg/L nAg suspension, the antimicrobial effect of silver was mitigated by the addition of 3.0 mg/L cysteine, which allowed bacterial growth. Similarly, when cysteine (27 mg/L) was placed in suspension with *P. mendocina* and the nAg-PSf membrane, the nearly 2-log inactivation of *P. mendocina* decreased to 60% (Figure 8.8).

Table 8.3: Growth of *P. mendocina* biofilm (sessile cells) and planktonic cells during three days. Microbial concentrations below are given as log(CFU/mL) with the standard deviation.

	Incubation Time		
	24 h	**48 h**	**72 h**
Polysulfone - Planktonic	8.45 ± 0.13	7.68 ± 0.37	7.85 ± 0.13
- Sessile	6.90 ± 0.05	6.22 ± 0.34	6.11 ± 0.58
nAg-polysulfone - Planktonic	0.67 ± 1.35	no growth	no growth
- Sessile	0.38 ± 0.76	0.5 ± 1.0	no growth

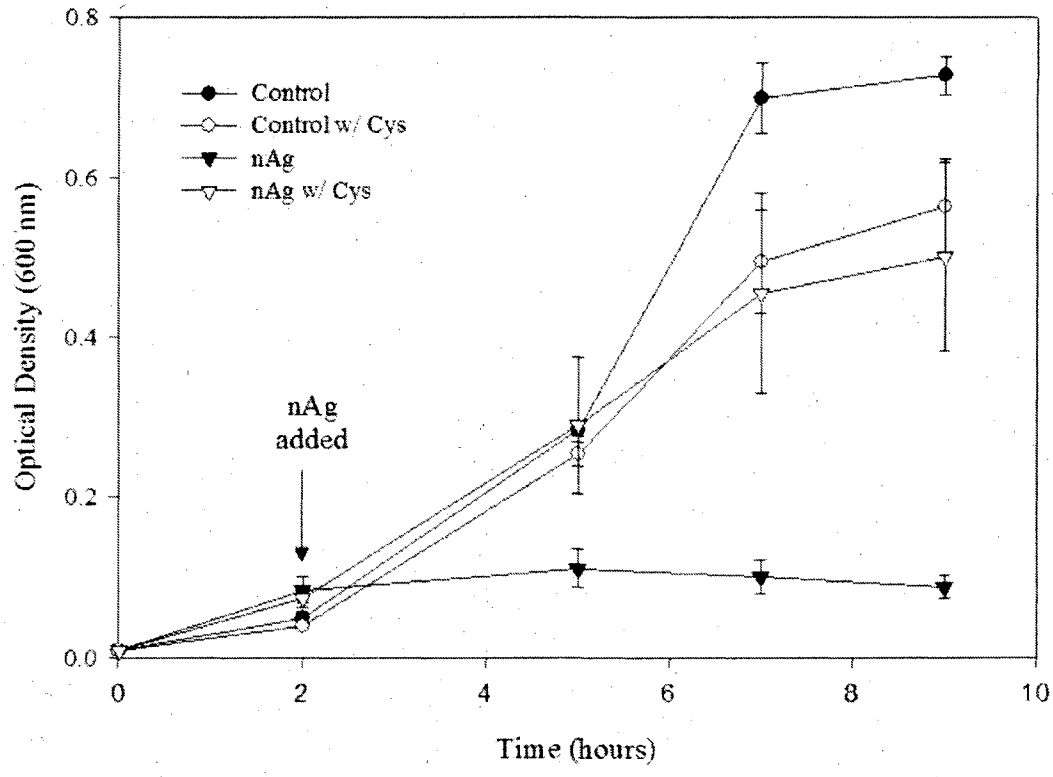

Figure 8.7: *E. coli* in suspension was inhibited by nAg (2.7 mg/L) unless cysteine (3.0 mg/L) was present. Suspension was spiked with nAg after two hours of incubation. Error bars represent 95% confidence intervals.

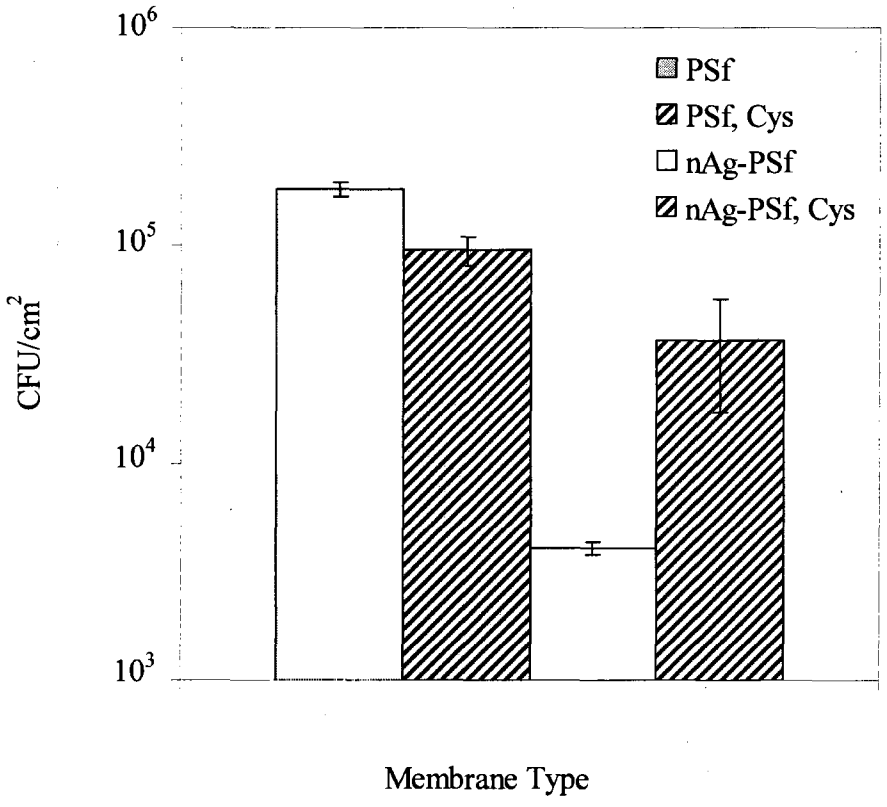

Figure 8.8: Inhibition of *P. mendocina* KR1 biofilm by nAg-PSf was prevented by 27 mg/L cysteine (cys). This graph depicts biofilm growth after four hours incubation in MD medium.

8.5 Enhanced virus removal by nAg-PSf membranes

Incorporation of nAg significantly enhanced virus removal by filtration. Influent concentrations of up to $5 \pm 0.2 \times 10^5$ PFU/mL were completely removed by filtration through nAg-PSf membranes. In contrast, viral concentrations greater than 10^2 PFU/mL were found in the filtrate of PSf membranes (Table 8.3). Although the exact mechanism of increased virus removal in this study remains unclear, various mechanisms were considered to explain virus removal, including size exclusion, depth filtration, electrostatic adsorption, and inactivation of viruses by Ag^+ ions.

While the nominal size of MS2 was 25 nm, our Dynamic Light Scattering (DLS) analyses indicated that the viruses were aggregated in solution, and the measured mean hydrodynamic diameter was 743 nm. Thus, it was likely that the larger aggregate size allowed some viruses to be removed by both PSf and nAg-PSf membranes through size exclusion.

Depth filtration was not a plausible cause for the increase in virus removal because the nAg-PSf membranes were significantly thinner than the PSf controls ($p < 0.05$, Table 8.1). The zeta potentials of both MS2 and the membrane were negative (-18.5 mV and -7.5 mV, respectively); however, enhanced adsorption to silver oxides present in membrane may have occurred. The surface isoelectric point for silver oxides is 10.4 (Chau and Porter, 1991). Therefore, the nAg surfaces were likely positively charged at pH 8.3, the pH at which the viruses were filtered. Previous studies have reported that oxides and hydroxides of iron and aluminum increased MS2 and poliovirus adsorption by decreasing the magnitude of negative charge at diatomaceous earth

surfaces (Farrah et al., 1991). The same effect may have been responsible for the increased virus removal due to the presence of silver oxides.

In addition to localized electrostatic adsorption, inactivation and/or irreversible adsorption of viruses may have contributed to enhanced viral removal by nAg-PSf membranes (Table 8.3). Inactivation of MS2 viruses by Ag^+ ions has been previously reported (Kim et al., 2008) and was corroborated in additional batch tests with a suspension of MS2 (10^9 PFU/mL) (Supplemental Information, Table 8.4). Interestingly, Ag^+ ions (18 mg/L) exerted significantly stronger antiviral activity (4-log removal after 1.5 h exposure) than an equivalent concentration of nAg particles, which released only 8 μg/L Ag^+ ions, causing no significant virus inactivation. This suggests that Ag^+ released from nAg may have accounted for some enhanced removal.

Table 8.3: Viral removal by membrane filtration. Plaque counts were performed on the influent and filtrates through PSf and nAg-PSf membranes. The values are expressed as average and standard deviation (n=4) (Zodrow et al., 2009).

Influent (PFU/mL)	PSf filtrate (PFU/mL)	nAg-PSf filtrate (PFU/mL)
$5 \pm 0.2 \times 10^5$	625 ± 35	0
$6 \pm 0.1 \times 10^4$	375 ± 148	0

Table 8.4: Viruses were inactivated by Ag^+ ions but not by nAg particles. Total silver that was incorporated into nAg-PSf membranes was introduced to viruses in the form of $AgNO_3$ salt solution and nAg suspension. Only 8 μg/L Ag^+ ions were released from 18 mg/L nAg particles. The values are expressed as average and standard deviation (n=4).

Control (PFU/mL)	18 mg/L nAg (PFU/mL)	18 mg/L $AgNO_3$ (PFU/mL)
2.65×10^9	2.03×10^9	1.52×10^5

8.6 Technological challenges

Silver release from commercial products containing nAg is an ever-growing concern (Benn and Westerhoff, 2008). This calls for future research that leads to improved nAg incorporation protocols that ideally concentrate the particles on the selective layer of the membrane, anchoring or coating nAg to slow the release of silver ions. Potential approaches to be explored include encapsulating nAg in a polymer and then covalently binding it to membrane polymers either directly or through the use of cross-linkers. Another option may be to encapsulate the silver in a substance that is degraded by bacteria so it is released at a constant rate (Loher et al., 2008). Additionally, silver lost from the membrane could be regenerated through the reduction and deposition of silver salts, such as $AgNO_3$ (Deng et al., 2008).

In addition to rapid loss of silver from these membranes, future use of these membranes in water treatment must address two other potential challenges with membrane performance – bacterial resistance to heavy metals and water chemistry. To illustrate the first challenge, similar experiments were conducted with *P. aeruginosa*, a metal-resistant bacterium that contains a cation-antiporter efflux pump (Hassen et al., 2001) that showed no decreases in bacteria growth (Figure 8.9). It is also very likely that the effectiveness of nAg-PSf membranes will be influenced by the composition of the water to which they are exposed. Silver toxicity to *E. coli* is altered by common water constituents that affect silver solubility and bioavailability, such as chloride, phosphates, sulfides, DOC, and compounds containing thiol groups. These compounds decrease the potency of silver ions and, in the case of cysteine, can reverse some of the damage to bacteria cells caused by silver (Russell and Hugo, 1994; Gupta and Silver, 1998; Butkus

et al., 2005). Bactericidal action of silver ions also increases with increasing temperature and pH (Russell and Hugo, 1994), which are two important factors in water treatment process control.

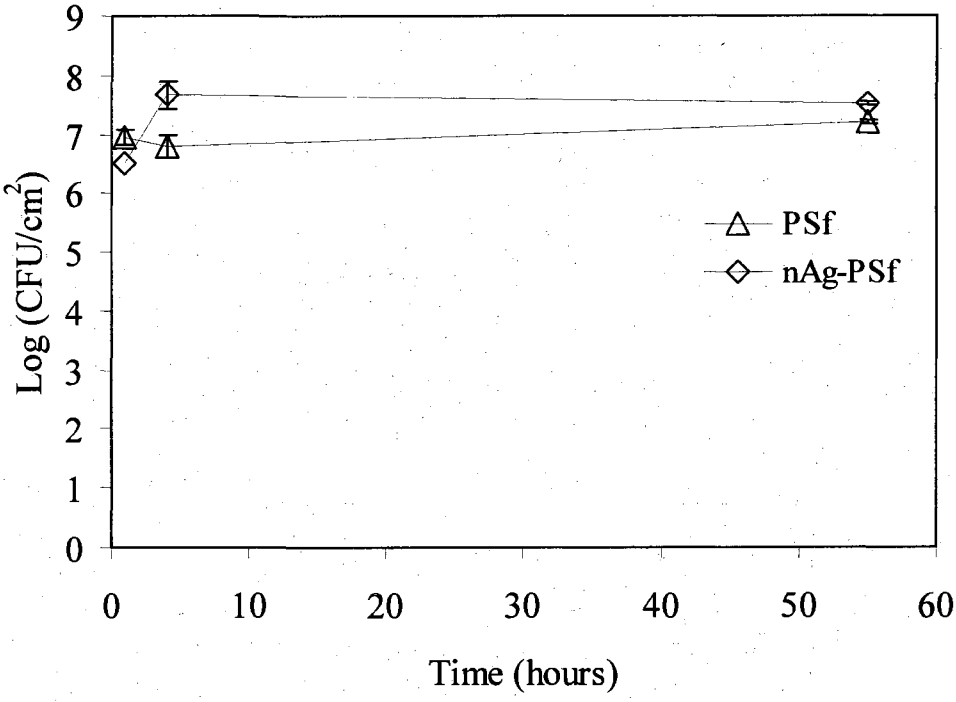

Figure 8.9: Biofilm growth of metal-resistant *P. aeruginosa* was not affected by the nAg-PSf membrane.

9.0 CONCLUSIONS, ENGINEERING SIGNIFICANCE, AND FUTURE RESEARCH NEEDS

The use of silver-impregnated antimicrobial materials is rapidly increasing, and the potential for silver to solve the biofouling problem and enhance virus removal in water filtration membranes is worthy of consideration. We show in this study that nAg-PSf membranes were effective against two strains of bacteria – *E. coli* K12 and *P. mendocina* KR1, and that the antimicrobial activity was primarily due to the release of Ag^+ ions. Not only were these membranes antimicrobial, but they also prevented bacteria attachment to the membrane surface and reduced biofilm formation. Additionally, nAg-PSf membranes showed a significant improvement in virus removal, potentially though virus adsorption to the membrane or inactivation by virus by Ag^+.

In order to take advantage of nAg-enhanced membrane properties, nAg does not need to be embedded during the membrane preparation process. It can be added to a commercial membrane and regenerated as needed. However, two significant challenges to long-term performance of nAg-embedded membranes were apparent: loss of antimicrobial and antiviral activity due to depletion of silver from the membrane surface and ineffectiveness against silver-resistant bacterial strains. Rapid silver depletion could be addressed by future research focusing on better nAg fixation techniques that concentrate the silver near the surface of the membrane (where it is most effective) and encapsulate the silver to slow the release rate. Because eventual silver depletion may be

unavoidable, the effectiveness of nAg regeneration by reductive deposition of silver salts should be further explored (Chou et al., 2005; Deng et al., 2008). While nAg-impregnated membranes would not guarantee protection against silver-resistant bacteria strains, they may ensure antimicrobial activity against a wide variety of bacteria and viruses and provide long-term protection against biofouling and viral penetration of water filtration membranes.

The fabrication of a biofouling-resistant membrane would greatly improve membrane water treatment. This type of membrane could reduce or eliminate the need for pre-treatment or cleaning with hazardous chemicals. Biofouling reduction would also decrease flux decline and prolong membrane life. Although the addition of nanosilver has not been shown to decrease other types of fouling (namely by particles and minerals), it is likely that solutions for these problems could be developed, potentially through the addition of other materials into low-pressure membranes.

The up to 5-log removal of viruses by low-pressure membranes impregnated with nanosilver is of particular interest to the water filtration industry. Removal rates of this magnitude were previously thought only to be obtainable by higher pressure membranes (that remove viruses through size exclusion) or coagulation pre-treatment. These findings indicate that nanosilver filters could be used in much smaller systems (for example, in a hand-pump filter) to remove viruses without pre-treatment.

The combined benefit of nAg addition to polysulfone membranes – virus removal and biofouling reduction – provides a very strong argument for continued research in this area. Specifically, the following issues must be addressed:

- Concentration of nAg on the membrane surface

- Optimization of nAg addition (i.e., How much is silver enough?)
- Control of Ag^+ release rate (i.e., High enough to exert antimicrobial activity but not too high to prevent rapid depletion of silver?)
- Capture and reuse of leached silver ions
- Further characterization of virus removal mechanisms

Once these issues have been addressed, it is possible that nAg addition to water filtration membranes will be widely use to improve the long-term efficacy of water filtration membranes.

10.0 REFERENCES

2007. Membrane filtration technologies tackle water reuse and purification. Membrane Technology 2007, 9-11.

Amy, G., 2008. Fundamental understanding of organic matter fouling of membranes. Desalination 231, 44-51.

Arkhangelsky, E., Gitis, V., 2008. Effect of transmembrane pressure on rejection of viruses by ultrafiltration membranes. Sep. Purif. Technol. 62, 619-628.

Bellara, S.R., Cui, Z.F., MacDonald, S.L., Pepper, D.S., 1998. Virus removal from bioproducts using ultrafiltration membranes modified with latex particle pretreatment. Bioseparation 7, 79-88.

Benn, T.M., Westerhoff, P., 2008. Nanoparticle silver released into water from commercially available sock fabrics. Environ Sci Technol 42, 4133-4139.

Bosetti, M., Masse, A., Tobin, E., Cannas, M., 2002. Silver coated materials for external fixation devices: in vitro biocompatibility and genotoxicity. Biomaterials 23, 887-892.

Brady-Estevez, A.S., Kang, S., Elimelech, M., 2008. A single-walled-carbon-nanotube filter for removal of viral and bacterial pathogens. Small 4, 481-484.

Brunet, L., Lyon, D.Y., Zodrow, K., Rouch, J.C., Caussat, B., Serp, P., Remigy, J.C., Wiesner, M.R., Alvarez, P.J.J., 2008. Properties of membranes containing semi-dispersed carbon nanotubes. Environ Eng Sci 25, 565-575.

Butkus, M.A., Talbot, M., Labare, M.P., 2005. Feasibility of the silver-UV process for drinking water disinfection. Water Res 39, 4925-4932.

Chau, L.K., Porter, M.D., 1991. Surface Isoelectric Point of Evaporated Silver Films - Determination by Contact-Angle Titration. J Colloid Interf Sci 145, 283-286.

Chellam, S., Xu, W.D., 2006. Blocking laws analysis of dead-end constant flux microfiltration of compressible cakes. J Colloid Interf Sci 301, 248-257.

Cheryan, M., 1998. Ultrafiltration and microfiltration handbook. Technomic Pub. Co., Lancaster, Pa., pp. xvii, 527 p.

Chou, W.L., Yu, D.G., Yang, M.C., 2005. The preparation and characterization of silver-loading cellulose acetate hollow fiber membrane for water treatment. Polym Advan Technol 16, 600-607.

Corrias, M., Caussat, B., Ayral, A., Durand, J., Kihn, Y., Kalck, P., Serp, P., 2003. Carbon nanotubes produced by fluidized bed catalytic CVD: first approach of the process. Chem Eng Sci 58, 4475-4482.

Cunningham, J.H., Cunningham, C., Van Aken, B., Lin, L.S., 2008. Feasibility of disinfection kinetics and minimum inhibitory concentration determination on bacterial cultures using flow cytometry. Water Sci Technol 58, 937-944.

Damm, C., Munsted, H., Rosch, A., 2007. Long-term antimicrobial polyamide 6/silver-nanocomposites. Journal of Materials Science 42, 6067-6073.

Davies, R.L., Etris, S.F., 1997. The development and functions of silver in water purification and disease control. Catalysis Today 36, 107-114.

de Prijck, K., Nelis, H., Coenye, T., 2007. Efficacy of silver-releasing rubber for the prevention of *Pseudomonas aeruginosa* biofilm formation in water. Biofouling 23, 405-411.

Deng, Y.Q., Dang, G.D., Zhou, H.W., Rao, X.H., Chen, C.H., 2008. Preparation and characterization of polyimide membranes containing Ag nanoparticles in pores distributing on one side. Materials Letters 62, 1143-1146.

Ding, J.W., Liu, C.P., 2005. Tube geometry effects on quantum transport in carbon nanotube electron resonators. Int J Mod Phys B 19, 3301-3307.

Elechiguerra, J.L., Burt, J.L., Morones, J.R., Camacho-Bragado, A., Gao, X., Lara, H.H., Yacaman, M.J., 2005. Interaction of silver nanoparticles with HIV-1. J Nanobiotechnology 3, 6.

Fang, J.S., Lyon, D.Y., Wiesner, M.R., Dong, J.P., Alvarez, P.J.J., 2007. Effect of a fullerene water suspension on bacterial phospholipids and membrane phase behavior. Environ Sci Technol 41, 2636-2642.

Farrah, S.R., Preston, D.R., Toranzos, G.A., Girard, M., Erdos, G.A., Vasuhdivan, V., 1991. Use of Modified Diatomaceous-Earth for Removal and Recovery of Viruses in Water. Applied and Environmental Microbiology 57, 2502-2506.

Feng, Q.L., Wu, J., Chen, G.Q., Cui, F.Z., Kim, T.N., Kim, J.O., 2000. A mechanistic study of the antibacterial effect of silver ions on *Escherichia coli* and *Staphylococcus aureus*. J Biomed Mater Res 52, 662-668.

Fievet, P., Sbai, M., Szymczyk, A., Vidonne, A., 2003. Determining the zeta-potential of plane membranes from tangential streaming potential measurements: effect of the membrane body conductance. J Membrane Sci 226, 227-236.

Fortner, J.D., Lyon, D.Y., Sayes, C.M., Boyd, A.M., Falkner, J.C., Hotze, E.M., Alemany, L.B., Tao, Y.J., Guo, W., Ausman, K.D., Colvin, V.L., Hughes, J.B., 2005. C-60 in water: Nanocrystal formation and microbial response. Environ Sci Technol 39, 4307-4316.

Gogoi, S.K., Gopinath, P., Paul, A., Ramesh, A., Ghosh, S.S., Chattopadhyay, A., 2006. Green fluorescent protein-expressing *Escherichia coli* as a model system for investigating the antimicrobial activities of silver nanoparticles. Langmuir 22, 9322-9328.

Gupta, A., Silver, S., 1998. Silver as a biocide: will resistance become a problem? . Nature Biotechnology 16, 888.

Hanft, S., 2006. Membrane Microfiltration Market. BCC Research MST028C.

Hassen, A., Jerboui, Z., Cherif, M., Saidi, N., Gharbi, S., Boudabous, A., 2001. Impact of heavy metals on the selective phenotypical markers of *Pseudomonas aeruginosa*. Microbial Ecol 42, 99-107.

Huang, C.T., Yu, F.P., Mcfeters, G.A., Stewart, P.S., 1995. Nonuniform Spatial Patterns of Respiratory Activity within Biofilms during Disinfection. Applied and Environmental Microbiology 61, 2252-2256.

Hwang, E.T., Lee, J.H., Chae, Y.J., Kim, Y.S., Kim, B.C., Sang, B.I., Gu, M.B., 2008. Analysis of the toxic mode of action of silver nanoparticles using stress-specific bioluminescent bacteria. Small 4, 746-750.

Jayasekara, N.Y., Heard, G.M., Cox, J.M., Fleet, G.H., 1999. Association of micro-organisms with the inner surfaces of bottles of non-carbonated mineral waters. Food Microbiology 16, 115-128.

Jirage, K.B., Hulteen, J.C., Martin, C.R., 1998. Chemical selectivity in gold nanotubular membranes. Abstr Pap Am Chem S 216, U306-U306.

Kang, S., Herzberg, M., Rodrigues, D.F., Elimelech, M., 2008. Antibacterial effects of carbon nanotubes: Size does matter. Langmuir 24, 6409-6413.

Kang, S.W., Kim, J.H., Char, K., Won, J., Kang, Y.S., 2006. Nanocomposite silver polymer electrolytes as facilitated olefin transport membranes. Journal of Membrane Science 285, 102-107.

Kaye, G.W.C., Laby, T.H., 1986. Tables of physical and chemical constants and some mathematical functions. Longman, London ; New York.

Kennedy, J.E., Wei, C.I., Oblinger, J.L., 1986. Methodology for Enumeration of Coliphages in Foods. Applied and Environmental Microbiology 51, 956-962.

Kim, J.Y., Lee, C., Cho, M., Yoon, J., 2008. Enhanced inactivation of E. coli and MS-2 phage by silver ions combined with UV-A and visible light irradiation. Water Res 42, 356-362.

Kimura, K., Maeda, T., Yamamura, H., Watanabe, Y., 2008. Irreversible membrane fouling in microfiltration membranes filtering coagulated surface water. J Membrane Sci 320, 356-362.

Lam, C.W., James, J.T., McCluskey, R., Arepalli, S., Hunter, R.L., 2006. A review of carbon nanotube toxicity and assessment of potential occupational and environmental health risks. Crit Rev Toxicol 36, 189-217.

Li, Q., Mahendra, S., Lyon, D.Y., Brunet, L., Liga, M.V., Li, D., Alvarez, P.J.J., 2008. Antimicrobial Nanomaterials for Water Disinfection and Microbial Control: Potential Applications and Implications. (in press).

Liau, S.Y., Read, D.C., Pugh, W.J., Furr, J.R., Russell, A.D., 1997. Interaction of silver nitrate with readily identifiable groups: relationship to the antibacterial action of silver ions. Lett Appl Microbiol 25, 279-283.

Loher, S., Schneider, O.D., Maienfisch, T., Bokorny, S., Stark, W.J., 2008. Micro-organism-triggered release of silver nanoparticles from biodegradable oxide carriers allows preparation of self-sterilizing polymer surfaces. Small 4, 824-832.

Lovins, W.A., Taylor, J.S., Hong, S.K., 2002. Micro-organism rejection by membrane systems. Environ Eng Sci 19, 453-465.

Lyon, D.Y., Adams, L.K., Falkner, J.C., Alvarez, P.J.J., 2006. Antibacterial activity of fullerene water suspensions: Effects of preparation method and particle size. Environ Sci Technol 40, 4360-4366.

Lyon, D.Y., Fortner, J.D., Hughes, J.B., Alvarez, P.J., 2005a. Impact of a C-60 water suspension on bacteria. Abstr Pap Am Chem S 229, U910-U910.

Lyon, D.Y., Fortner, J.D., Sayes, C.M., Colvin, V.L., Hughes, J.B., 2005b. Bacterial cell association and antimicrobial activity of a C-60 water suspension. Environmental Toxicology and Chemistry 24, 2757-2762.

Mauter, M.S., Elimelech, M., 2008. Environmental applications of carbon-based nanomaterials. Environ Sci Technol 42, 5843-5859.

Mcdonogh, R., Schaule, G., Flemming, H.C., 1994. The Permeability of Biofouling Layers on Membranes. Journal of Membrane Science 87, 199-217.

Morancais, A., Caussat, B., Kihn, Y., Kalck, P., Plee, D., Gaillard, P., Bernard, D., Serp, P., 2007. A parametric study of the large scale production of multi-walled carbon

nanotubes by fluidized bed catalytic chemical vapor deposition. Carbon 45, 624-635.

Morones, J.R., Elechiguerra, J.L., Camacho, A., Holt, K., Kouri, J.B., Ramirez, J.T., Yacaman, M.J., 2005. The bactericidal effect of silver nanoparticles. Nanotechnology 16, 2346-2353.

Mulder, M., 1990. Basic Principles of Membrane Technology. Kluwer Academic Publishers, Norwell, MA, U.S.A.

Narayan, R.J., Berry, C.J., Brigmon, R.L., 2005. Structural and biological properties of carbon nanotube composite films. Mat Sci Eng B-Solid 123, 123-129.

Navarro, E., Piccapietra, F., Wagner, B., Marconi, F., Kaegi, R., Odzak, N., Sigg, L., Behra, R., 2008. Toxicity of Silver Nanoparticles to Chlamydomonas reinhardtii. Environ. Sci. Technol.

Nicolaisen, B., 2003. Developments in membrane technology for water treatment. Desalination 153, 355-360.

Oka, Y., Kim, W.C., Yoshida, T., Hirashima, T., Mouri, H., Urade, H., Itoh, Y., Kubo, T., 2008. Efficacy of titanium dioxide photocatalyst for inhibition of bacterial colonization on percutaneous implants. J Biomed Mater Res B 86B, 530-540.

Ong, S.L., Hu, J.Y., Biryulin, Y.F., Polotskaya, G.A., 2006. Fullerene-containing polymer membranes for rejection of estrogenic compounds in water. Fuller Nanotub Car N 14, 463-466.

Pal, S., Tak, Y.K., Song, J.M., 2007. Does the Antibacterial Activity of Silver Nanoparticles Depend on the Shape of the Nanoparticle? A Study of the Gram-Negative Bacterium *Escherichia coli*. Applied and Environmental Microbiology 73, 1712-1720.

Panacek, A., Kvitek, L., Prucek, R., Kolar, M., Vecerova, R., Pizurova, N., Sharma, V.K., Nevecna, T., Zboril, R., 2006. Silver colloid nanoparticles: Synthesis, characterization, and their antibacterial activity. Journal of Physical Chemistry B 110, 16248-16253.

Polotskaya, G.A., Penkova, A.V., Toikka, A.M., Pientka, Z., Brozova, L., Bleha, M., 2007. Transport of small molecules through polyphenylene oxide membranes modified by fullerene. Separ Sci Technol 42, 333-347.

Ratte, H.T., 1999. Bioaccumulation and toxicity of silver compounds: A review. Environ Toxicol Chem 18, 89-108.

Ridgway, H., Ishida, K., Rodriguez, G., Safarik, J., Knoell, T., Bold, R., 1999. Biofouling of membranes: Membrane preparation, characterization, and analysis of bacterial adhesion. Biofilms 310, 463-494.

Rogers, J.V., Parkinson, C.V., Choi, Y.W., Speshock, J.L., Hussain, S.M., 2008. A preliminary assessment of silver nanoparticle inhibition of monkeypox virus plaque formation. Nanoscale Res Lett 3, 129-133.

Rojas-Chapana, J., Troszczynska, J., Firkowska, I., Morsczeck, C., Giersig, M., 2005. Multi-walled carbon nanotubes for plasmid delivery into Escherichia coli cells. Lab Chip 5, 536-539.

Russell, A.D., Hugo, W.B., 1994. Antimicrobial activity and action of silver. Prog Med Chem 31, 351-370.

Santos, E., Avalle, L.B., Scurtu, R., Jones, H., 2007. l-Cysteine films on Ag(1 1 1) investigated by electrochemical and nonlinear optical methods. Chemical Physics 342, 236-244.

Savage, N., Diallo, M.S., 2005. Nanomaterials and water purification: Opportunities and challenges. J Nanopart Res 7, 331-342.

Sayes, C.M., Liang, F., Hudson, J.L., Mendez, J., Guo, W.H., Beach, J.M., Moore, V.C., Doyle, C.D., West, J.L., Billups, W.E., Ausman, K.D., Colvin, V.L., 2006. Functionalization density dependence of single-walled carbon nanotubes cytotoxicity in vitro. Toxicol Lett 161, 135-142.

Silver, S., Phung, L.T., 1996. Bacterial heavy metal resistance: New surprises. Annu Rev Microbiol 50, 753-789.

Sondi, I., Salopek-Sondi, B., 2004. Silver nanoparticles as antimicrobial agent: a case study on *E. coli* as a model for Gram-negative bacteria. J Colloid Interf Sci 275, 177-182.

Thurston-Enriqueza, J.A., Haas, C.N., Jacangelo, J., Gerba, C.P., 2005. Inactivation of enteric adenovirus and feline calicivirus by ozone. Water Res 39, 3650-3656.

Trevors, J.T., 1987. Silver Resistance and Accumulation in Bacteria. Enzyme and Microbial Technology 9, 331-333.

Vrijenhoek, E.M., Hong, S., Elimelech, M., 2001. Influence of membrane surface properties on initial rate of colloidal fouling of reverse osmosis and nanofiltration membranes. J Membrane Sci 188, 115-128.

Wang, Z., Wu, Z., Yin, X., Tian, L., 2008. Membrane fouling in a submerged membrane bioreactor (MBR) under sub-critical flux operation: Membrane foulant and gel layer characterization. J Membrane Sci 325, 238-244.

WHO, 2004. Guidelines for Drinking Water Quality. World Health Organization Geneva, Switzerland.

Xu, J.J., Ao, Y.H., Fu, D.G., Lin, J., Lin, Y.H., Shen, X.W., Yuan, C.W., Yin, Z.D., 2008. Photocatalytic activity on TiO2-coated side-glowing optical fiber reactor under solar light. J Photoch Photobio A 199, 165-169.

Xu, X.H., Brownlow, W.J., Kyriacou, S.V., Wan, Q., Viola, J.J., 2004. Real-time probing of membrane transport in living microbial cells using single nanoparticle optics and living cell imaging. Biochemistry 43, 10400-10413.

Yahya, M.T., Straub, T.M., Gerba, C.P., 1992. Inactivation of Coliphage-Ms-2 and Poliovirus by Copper, Silver, and Chlorine. Can J Microbiol 38, 430-435.

Yavuz, C.T., Mayo, J.T., Yu, W.W., Prakash, A., Falkner, J.C., Yean, S., Cong, L.L., Shipley, H.J., Kan, A., Tomson, M., Natelson, D., Colvin, V.L., 2006. Low-field magnetic separation of monodisperse Fe3O4 nanocrystals. Science 314, 964-967.

Zhu, B.T., Clifford, D.A., Chellam, S., 2005. Virus removal by iron coagulation-microfiltration. Water Res 39, 5153-5161.

Zodrow, K., Brunet, L., Mahendra, S., Li, D., Zhang, A., Li, Q.L., Alvarez, P.J.J., 2009. Polysulfone ultrafiltration membranes impregnated with silver nanoparticles show improved biofouling resistance and virus removal. Water Res 43, 715-723.

APPENDIX: SUPPLEMENTAL INFORMATION

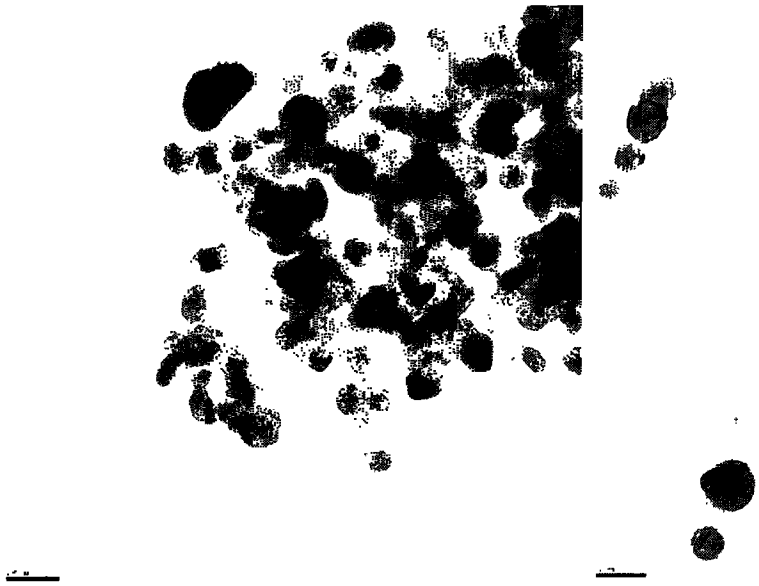

Figure A1: Images of silver nanoparticles (purchased from Novacentrix; Austin, TX) dispersed in DI water and dried on a copper grid. The scale bar indicates 50 nm.

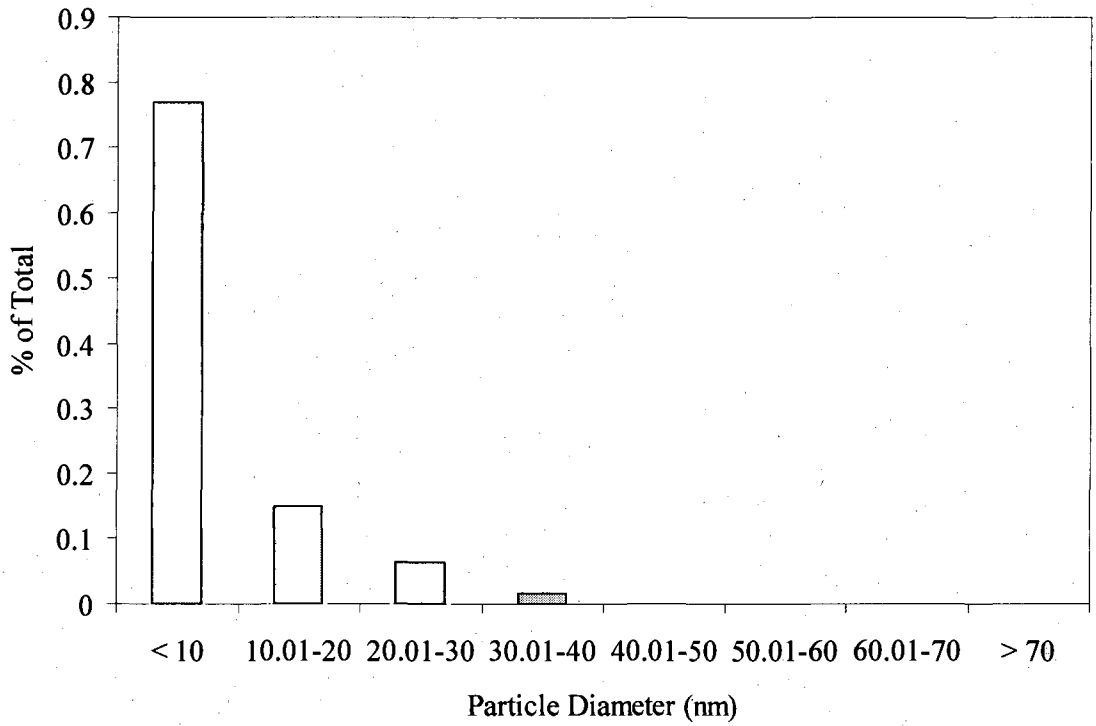

Figure A2: Although the nAg distribution was bimodal (with another peak at approximately 50 nm), these larger particles tended to aggregate (see Figure A1), making quantification difficult. Thus, this depiction distribution favors the smaller particles.

Table A1: Data depicted in Figure 4.3; cumulative silver lost from membrane with filtration.

		Cumulative Mass Silver lost per cm2 (ug)					
Volume Filtered (mL)	**Volume Filtered (L/cm2)**	**Mass 1**	**Mass 2**	**Mass 3**	**Average**	**SD**	**CI95**
0	0				0	0	0
100	0.010697245	0.3851	0.3851	0.33161	0.36727	0.0268	0.01662
600	0.064183468	1.9362	2.04317	2.09666	2.02534	0.09047	0.05609
1100	0.117669691	1.9362	2.25712	2.3106	2.16797	0.12191	0.07558
1600	0.171155914	2.20363	2.47106	2.52455	2.39975	0.06789	0.04209
2100	0.224642138	2.41758	2.68501	2.73849	2.61369	0.03782	0.02345
2600	0.278128361	2.47106	2.68501	2.79198	2.64935	0.03566	0.02211
3100	0.331614584	2.52455	2.68501	2.84547	2.68501	0.0598	0.03708

Table A2: Data depicted in Figure 4.1(a); loss of used membrane effectiveness against *E. coli K12*. Growth was measured using the optical density of the suspension at 600 nm.

Time (h)	PSf 1	PSf 2	nAg-PSf 1	nAg-PSf 2	low nAg-PSf 1	low nAg-PSf 2
3	0.000	0.001	0.000	0.000	0.000	0.000
5.5	0.128	0.007	0.000	0.000	0.034	0.000
9.5	0.283	0.171	0.007	0.000	0.251	0.007
16.5	0.303	0.205	0.003	0.001	0.211	0.046
23	0.429	0.313	0.010	0.000	0.170	0.397
30	0.587	0.482	0.000	0.000	0.144	0.298

Table A3: Data depicted in Figure 4.1(b); Loss of used membrane effectiveness against *P. mendocina KR1*. Growth was measured using the optical density of the suspension at 600 nm.

Time (h)	PSf 1	PSf 2	nAg-PSf 1	nAg-PSf 2	low nAg-PSf
3	0.004	0.003	0.000	0.000	0.000
5.5	0.043	0.020	0.000	0.021	0.000
9.5	0.316	0.235	0.002	0.003	0.01
16.5	0.402	0.301	0.000	0.000	0.405
23	0.430	0.499	0.015	0.005	0.552
30	0.460	0.428	0.009	0.000	0.548

Table A4: Data depicted in Figure 4.5(a); bacteria survival after filtration-deposition onto membrane surface

Sample	PSf	nAg-PSf
1	15	0
2	8	1
3	20	0

Table A5: Data depicted in Figure 4.5(b); bacteria attachment to membrane surface

Sample	PSf	nAg-PSf
1	6525	549
2	7761	343
3	14217	824
4	12706	343
5	7212	481
6	4052	412
7	10234	481
8	4464	481
9		412
10		343

Table A6: Data depicted in Figure 4.7; inhibition of bacteria in suspension by nAg and AgNO3 with and without cysteine.

Time (h)	Cys	no Cys	nAg	$AgNO_3$	nAg + Cys	$AgNO_3$ + Cys
0	0.01	0.01	0.01	0.01	0.01	0.01
1	0.019	0.021	0.032	0.063	0.03	0.071
2	0.055	0.056	0.08	0.288	0.079	0.158
3	0.153	0.148	0.105	0.138	0.219	0.142
4	0.375	0.356	0.089	0.125	0.446	0.132
5	0.535	0.595	0.079	0.114	0.621	0.126
6	0.623	0.716	0.081	0.111	0.681	0.121
7	0.629	0.784	0.071	0.107	0.684	0.119

Table A7: Data depicted in Figure 4.8; inhibition of biofilm growth on PSf and nAg-PSf membranes in the presence of cysteine (4 hours). CFU/cm2 are displayed.

Sample	PSf	nAg-PSf	PSf w/ Cys	nAg-PSf w/ Cys
1	179000	3900	104000	47000
2	183200	4200	96000	39000
3		4100	87000	24000

Table A8: Data depicted in Figure 4.9; biofilm of *P. aeruginosa* was not inhibited by the nAg-PSf membrane

	Biofilm Growth (log(CFU/cm^2))			
Time	**PSf 1**	**PSf 2**	**nAg-PSf 1**	**nAg-PSf 2**
1 hour	7.3	7.2	6.8	n.d.
4 hours	7.2	7.0	7.8	8.1
24 hours	n.d.	n.d.	n.d.	n.d.
55 hours	7.5	7.5	7.8	7.8